ELECTRON SPIN RESONANCE STUDIES OF SMALL FREE RADICALS TRAPPED IN INERT MATRICES AT 4.2°K.

by

MICHAEL CHARLES LEWIS GERRY
B.A., UNIVERSITY OF BRITISH COLUMBIA, 1960

A THESIS SUBMITTED IN PARTIAL FULFILMENT
OF THE REQUIREMENTS FOR THE DEGREE OF
MASTER OF SCIENCE

in the Department
of
CHEMISTRY

We accept this thesis as conforming to
the required standard

THE UNIVERSITY OF BRITISH COLUMBIA
August, 1962.

In presenting this thesis in partial fulfilment of the requirements for an advanced degree at the University of British Columbia, I agree that the Library shall make it freely available for reference and study. I further agree that permission for extensive copying of this thesis for scholarly purposes may be granted by the Head of my Department or by his representatives. It is understood that copying or publication of this thesis for financial gain shall not be allowed without my written permission.

Department of CHEMISTRY

The University of British Columbia,
Vancouver 8, Canada.

Date AUGUST 28, 1962

ABSTRACT

Small free radicals trapped in solid argon, krypton and carbon tetrachloride at 4.2°K have been studied using electron spin resonance (ESR).

An attempt was made to determine whether the methylene radical, produced by the photolysis of diazomethane and ketene trapped in the solid matrix, has a triplet ground state. No signal definitely attributable to the methylene radical was observed. It is postulated that the zero field splitting due to the spin-spin coupling of the unpaired electrons broadened any ESR signal beyond detectability. The ESR signal of trapped methyl radicals was observed in some experiments, and it is suggested that they were formed by abstraction of hydrogen atoms from another deposited material by methylene radicals. An experiment in which diazomethane was photolysed in the presence of D_2O in an argon matrix at 4.2°K yielded an ESR signal which may possibly have been due to the CH_2D radical.

An investigation has been carried out of the populations of the rotational levels of methyl radicals produced by the photolysis of trapped methyl iodide and dimethyl mercury at 4.2°K. For thermal equilibrium freely rotating radicals should populate only the ground state at this temperature, but it was found that the lowest two levels were both populated. It is suggested that either there was

not thermal equilibrium, or, more likely, the methyl radicals were undergoing hindered rotation.

Room temperature equilibrium mixtures of N_2F_4 - NF_2 were trapped in the three matrices at 4.2°K, and ESR absorption due to the trapped NF_2 radicals was observed. Three lines were observed at this temperature, with the centre one of greater amplitude and smaller line width than the outer two. During warmup the amplitudes and widths of these lines became approximately equal and two further triplets appeared, symmetrically distributed about the centre line. From the warmup spectra the isotropic hyperfine splitting constants for fluorine and nitrogen have been deduced to be 168 and 48 mc./sec. respectively. It is suggested that the radicals underwent slow isotropic rotation at 4.2°K. The degree of s-character of the molecular orbital containing the unpaired electron is discussed in the light of the isotropic hyperfine splitting constants. An unsuccessful attempt to find hyperfine and rotational structure in the ESR signal of the NF_2 radical in the gas phase was carried out.

The photolysis of CF_3I in krypton and carbon tetrachloride matrices at 4.2°K yielded a very complicated ESR spectrum. A phase reversal of some of the lines was observed. A broad single line was observed when CF_3I in carbon tetrachloride was irradiated at 77°K. At the time of writing no definite interpretation of the spectra can be suggested.

ACKNOWLEDGMENTS

Many thanks to Professor C.A. McDowell for his great interest and help in this work. To Dr. J.B. Farmer I am most grateful for his much needed guidance throughout the experiments. I also thank Mr. R. Muelchen and Mr. J. Sallos, who were always most helpful, especially at the times when things went wrong.

With many members of the Department of Chemistry I have had discussions on various matters concerning this research; I thank them very much. Also, many members of the department provided me with compounds; I am also grateful to them. Many thanks to Dr. J.A. Bell and Dr. C.B. Colburn for their communications. I must thank also the members of the technical staff of the department for their help.

I am grateful to the National Research Council of Canada for a Bursary (1960-61) and a Studentship (1961-62).

TABLE OF CONTENTS

LIST OF TABLES

LIST OF FIGURES

CHAPTER ONE.

GENERAL INTRODUCTION

1-1 Free Radicals at Low Temperatures.

Study of any chemical entity requires that there be present a sufficient quantity of that substance to give an observable signal on interaction with an appropriate measuring apparatus. For the case of a reactive species, of which most free radicals are excellent examples, obtaining such a quantity is often a major problem. It is usually solved either by producing the species in such large numbers that they may be studied before reacting (as in flash photolysis), or by preventing them from contacting anything with which they may react (as in matrix isolation).

In the experiments discussed in this thesis the latter method, matrix isolation, is used for study of small free radicals. The radicals are prevented from reacting by trapping them in a matrix of solid inert gas or another inert material. Rigidity of the matrix is necessary for effective trapping of the radicals, since a non-rigid matrix allows them to diffuse and hence recombine. Rigidity is achieved by reducing thermal motion of the atoms or molecules of the matrix material almost to zero with some coolant such as liquid nitrogen (b.p.77^{o}K) or liquid helium (b.p.4.2^{o}K); the refrigerant used will depend on the nature of the matrix. Studies by Pimentel and others (1) have shown that for effective trapping the temperature must be below about forty percent of the melting point of the matrix, and as liquid helium achieves this purpose adequately for the matrices used predominantly here (solid argon and krypton) it has been

used as the refrigerant.

Of the various methods used for studying trapped free radicals, electron spin resonance (ESR) is one of the most useful. In the first place, since the presence of an unpaired electron is necessary for ESR detection a trapped substance can be identified as a radical rather than a molecule with a closed shell. The nature of any coupling of the unpaired spin with other angular momenta (orbital momentum, nuclear spins, rotational motion) reveals much about the nature of the radical and its environment. Also, ESR can detect as few as 10^{12} radicals, an advantage of immense importance in studying species difficult to produce. The major disadvantage of ESR is the complexity and cost of the apparatus, but if this can be overcome the technique is excellent.

The work described in this thesis is rather similar to that carried out by the ESR group at the Johns Hopkins University (2)-(12). They obtain free radicals by depositing a mixture of matrix gas and decomposition products of a microwave discharge or ultraviolet irradiation on a sapphire needle at $4.2^{\circ}K$, or by irradiating a solid deposit of reagent and matrix with ultraviolet light. These workers have studied a number of species, including hydrogen (2)(6)(7)(8) and nitrogen (4)(5) atoms, amino (3) and alkyl (9) radicals as well as HCO (10), CN (12) and NO_2 (11), and have done much work interpreting their properties when trapped. The work described in this thesis extends the studies to various other radicals, whose ESR spectra are interpreted in

a similar fashion.

1-2 Basic Principles of Electron Spin Resonance

Electron spin resonance studies consist essentially of placing free radicals in a magnetic field and investigating transitions between Zeeman levels of any non compensated electron angular momenta. The Hamiltonian for such levels is:

$$\mathcal{H}_1 = g\beta \bar{H}.\bar{J} \tag{1}$$

where g = electronic g - factor; β = Bohr magneton; $\bar{H}$ = magnetic field; $\bar{J} = \bar{L} + \bar{S}$ = total angular momentum operator of the electrons; $\bar{L}$ = orbital angular momentum operator; $\bar{S}$ = spin angular momentum operator. In most free radicals $\bar{L} = 0$ so that $\mathcal{H}_1$ is written:

$$\mathcal{H}_1 = g\beta \bar{H} \cdot \bar{S} \tag{2}$$

In this case $g \approx 2$. In a strong magnetic field, which is usually the case in an ESR experiment, $\bar{S}$ is quantized along $\bar{H}$, so that if $\mathcal{H}_1$ is treated as a first order perturbation of the electronic potential and kinetic energies its energy levels are:

$$W_1 = M_S g\beta H_0 \tag{3}$$

where M_S = projection of the electron spin in the direction of $\bar{H}$; H_0 = the magnitude of the magnetic field. If S , the quantum number of the total spin, is $\frac{1}{2}$, equation (3) becomes:

$$W_1 = \pm \tfrac{1}{2} g\beta H_0 \tag{4}$$

The magnetic dipole selection rule $\Delta M_s = \pm 1$ allows transitions between the levels at energies of:

$$h\nu = g\beta H_0 \qquad (5)$$

where h = Planck's constant; ν = frequency. In actual fact these equations are applicable only when the radicals are in fairly rapid isotropic motion, for the g-factor has directional properties, and should be written as a tensor. Thus, equation (2) should read:

$$\mathcal{H}_1 = \beta \bar{H} \cdot \bar{\bar{G}} \cdot \bar{S} \qquad (6)$$

where $\bar{\bar{G}}$ is the g-factor tensor. $\bar{S}$ is nevertheless quantized in the field direction, so that equation (5) should be:

$$h\nu = \beta H_0 \left(\bar{\tau}_H \cdot \bar{\bar{G}} \cdot \bar{\tau}_H \right) \qquad (7)$$

where $\bar{\tau}_H$ is a unit vector in the field direction. However, when the radicals are in isotropic motion the g-factor term is constant for all sample orientations and equation (5) is applicable.

The following additional Hamiltonian, due to magnetic interactions of the nuclei in the radical, is superimposed on $\mathcal{H}_1$:

$$\mathcal{H}_2 = \sum_j \left(\bar{S} \cdot \bar{\bar{a}}_j \cdot \bar{I}_j + \gamma_j \bar{H} \cdot I_j \right) \qquad (8)$$

where $\bar{I}_j$ is the nuclear spin operator of nucleus j. The first term, due to the spin-spin interaction of the unpaired electron and nucleus j, is called the hyperfine (hf) interaction, and $\bar{\bar{a}}_j$ is called the hf interaction tensor. The second term is the

nuclear Zeeman energy which (as in this case) is often small enough to be neglected. $\gamma_j \bar{I}_j$ is the nuclear moment of nucleus j. The hyperfine interaction is written as a tensor because, like the g-factor, it has directional properties. Nevertheless $\bar{\bar{a}}_j$ may be subdivided into two parts:

$$\bar{\bar{a}}_j = A_j \bar{\bar{U}} + \bar{\bar{B}}_j \tag{9}$$

where $\bar{\bar{U}}$ is the unit dyadic. Equation (8) may be rewritten:

$$\begin{aligned} \mathcal{H}_2 &= \sum_j \left(A_j \bar{S} \cdot \bar{\bar{U}} \cdot \bar{I}_j + \bar{S} \cdot \bar{\bar{B}}_j \cdot \bar{I}_j \right) \\ &= \sum_j \left(A_j \bar{S} \cdot \bar{I}_j + \bar{S} \cdot \bar{\bar{B}}_j \cdot \bar{I}_j \right) \end{aligned} \tag{10}$$

A_j and $\bar{\bar{B}}_j$ are given by the following:

$$A_j = \frac{8\pi}{3} g \beta \gamma_j \delta(\bar{r}_j) \tag{11}$$

$$\bar{\bar{B}}_j = -g\beta \gamma_j \left[\frac{\bar{\bar{U}}}{r_j^3} - \frac{3 \bar{r}_j \bar{r}_j}{r_j^5} \right] \tag{12}$$

where r_j is the length of $\bar{r}_j$, the vector between nucleus j and the electron; $\delta(\bar{r}_j)$=Dirac delta function. It will be noted that A_j has no directional properties and is thus called the isotropic hf constant. Also $\delta(\bar{r}_j)$ requires that A_j=0 unless there is a finite probability of finding the electron at nucleus j, i.e. unless the orbital containing the unpaired electron has some s-character at nucleus j. $\bar{\bar{B}}_j$, which is traceless, does have directional character and is called the anisotropic hf interaction tensor.

Let us assume that the g-factor is isotropic and work in

a molecule - fixed coordinate system whose axes xyz are coincident with the principal axes of $\bar{\bar{B}}_j$. The hyperfine interaction superimposes an extra splitting on the electron Zeeman splitting, making the energy levels (13):

$$W = W_1 + W_{hf}$$

$$= M_S g\beta H_o + \sum_j M_S (M_I)_j \Big\{ A_j^2 + 2A_jB_j(3\cos^2\theta - 1) + C_j^2 \sin^2\theta \quad (13)$$
$$+ B_j^2(3\cos^2\theta + 1) + 2C_j(A_j - B_j)\sin^2\theta(\cos^2\chi - \sin^2\chi)\Big\}^{1/2}$$

where $(M_I)_j$ is the projection of $\bar{I}_j$ on the magnetic field; θ, Φ are spherical polar coordinates of the z-axis with respect to the external field; χ represents the orientation of the molecule about the z-axis; if B_{jx}, B_{jy}, B_{jz} are the three principal values of $\bar{\bar{B}}_j$, then:

$$\left.\begin{aligned} B_j &= \tfrac{1}{2} B_{jz} = -\tfrac{1}{2}(B_{jx} + B_{jy}) \\ C_j &= \tfrac{1}{2}(B_{jx} - B_{jy}) \end{aligned}\right\} \qquad (14)$$

B_j is called the anisotropic hf splitting constant. Note that for axial symmetry $B_{jx} = B_{jy}$ and $C_j = 0$, and equation (13) becomes:

$$W = M_S g\beta H_o + \sum_j M_S (M_I)_j \Big\{ A_j^2 + 2A_jB_j(3\cos^2\theta - 1) + B_j^2(3\cos^2\theta + 1)\Big\}^{1/2} \quad (15)$$

In the frequently found case of $|A_j| \gg |B_j|$, this becomes:

$$W = M_S g\beta H_o + \sum_j M_S (M_I)_j \Big\{ A_j + B_j(3\cos^2\theta - 1)\Big\} \qquad (16)$$

For spherical symmetry (including the case when the radicals are rotating at a frequency $\omega \gg \frac{B_j}{\hbar}$) (14), the anisotropic part

averages to zero, making the energy levels:

$$W = M_s g\beta H_o + \sum_j A_j M_s (M_I)_j \qquad (17)$$

Transitions occur according to the selection rules $\Delta M_s = \pm 1$, $\Delta (M_I)_j = 0$ at energies of:

$$h\nu = g\beta H_o + \sum_j A_j (M_I)_j \qquad (18)$$

These are shown schematically in Figure 1 for the case of $S = \frac{1}{2}, I_j$ (the quantum number of the total spin of nucleus j) $= \frac{1}{2}$. The equations show that the shift due to $\overline{\overline{B}}_j$ varies with the orientation of the radical in the magnetic field. If one is studying a sample containing randomly oriented radicals the main effect of $\overline{\overline{B}}_j$ is often to broaden the lines due to the isotropic hf interaction, sometimes changing their shape (16)(10), and other times making them undetectable.

The ESR transitions observed in these experiments involve the absorption of microwave power. The power absorbed is proportional to the population difference between the lower $\left(M_s = -\frac{1}{2}\right)$ and upper $\left(M_s = \frac{1}{2}\right)$ levels. Such a difference is usually found, since very often the spin system is in thermal equilibrium with its surroundings, and the populations of the levels follow a Boltzmann distribution. This distribution is maintained, even when microwave power is absorbed, by a mechanism (called spin-lattice relaxation) which depopulates the excited level fast enough to retain thermal equilibrium. Sometimes, however, the spin-lattice relaxation rate cannot keep up with the power absorption, so that the population difference, and hence the

To Follow Page 7

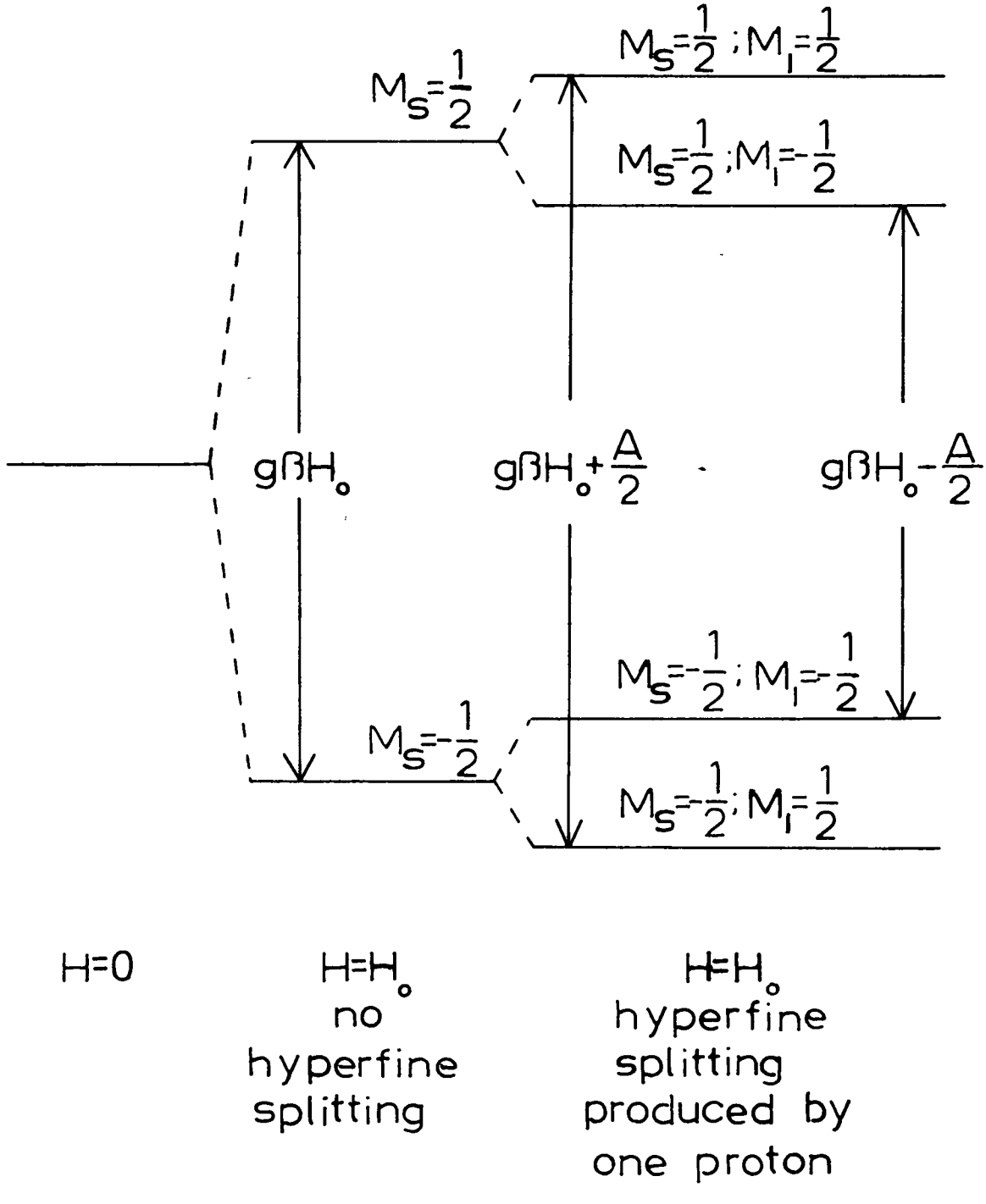

Figure 1. SPLITTING OF ELECTRONIC ENERGY LEVELS BY A MAGNETIC FIELD AND AN ISOTROPIC PROTON HYPERFINE INTERACTION.

power absorbed, decreases. A watch has to be kept for this phenomenon, called power saturation, especially at low temperatures, for it may wreak havoc with ESR measurements, broadening the absorption lines out of proportion.

CHAPTER TWO

GENERAL EXPERIMENTAL METHODS

2-1 Description of the Electron Spin Resonance Spectrometer

The X-band spectrometer, which was designed in this laboratory, uses a Varian V-153 klystron as a microwave source. Energy from the klystron enters a magic tee bridge connected on one side to a microwave cavity resonating in the TE_{012} mode and on the other to a resistive load; a silicon diode detector is connected to the third arm. With the detector as an indicator the klystron cavity size and reflector voltage are adjusted until power absorbed in the cavity is balanced by that absorbed in the resistive load. Finally, by setting up a slight inbalance with an attenuator in the resistive load arm a bias current of ca.100 microamperes is passed through the detector to increase the signal-to-noise ratio. The klystron frequency is locked to that of the cavity by an automatic frequency control (AFC) with a carrier channel of 10 kc./sec. Further attenuators in the waveguide system, one between the klystron and the magic tee, and the other between the magic tee and the cavity, allow the microwave power to the cavity to be reduced to one milliwatt and below. In the microwatt range the AFC works only with difficulty, so the resistive load can be replaced by another cavity to which the AFC can be connected at a high power level while the cavity containing the sample is operated at a low power level. The microwave frequency is measured with a Hewlett Packard 524/525/540 frequency counter, and the microwave power is monitored with a thermistor and a Hewlett Packard 430 power meter.

The magnetic field is produced by a Varian six-inch electromagnet with a 2.5 inch pole gap, and fitted with ring shim pole caps. It is measured with a proton resonance magnetometer. The latter consists of a 3 mm. probe coil containing glycerol, which is inserted into the magnet gap beside the cavity, and is connected to a marginal oscillator which is frequency modulated at 20 cycles/sec. The proton resonance signal is displayed on an oscilloscope and a signal generator loosely coupled to the oscillator is tuned to zero beat; the frequency of the generator is then measured with the counter. The magnetic field is modulated at 400 cycles/sec. or 20 cycles/sec. with a pair of auxiliary coils mounted round the cavity and signals are recorded as first derivatives of magnetic susceptibility vs. magnetic field. The very high signal-to-noise ratio in the spectrometer is due to the use of narrow band amplification techniques.

Block diagrams of the detection and AFC systems are in Figures 2 and 3.

2-2 The Liquid Helium Dewar System

The liquid helium dewar is based on the design of Duerig and Mador (16), and is shown in cross section in Figure 4. The centre container holds the liquid helium and is shielded by liquid nitrogen; the vacuum envelope is pumped to 10^{-7}-10^{-8} mm.Hg with an oil diffusion pump and a rotary oil pump, and the pressure in the system is measured with an NRC type 507 ionization gauge. The microwave cavity is attached directly to the liquid helium container, and in its centre is an 0.15 inch sapphire rod on which gaseous samples are condensed. In order to minimize

To Follow Page 10

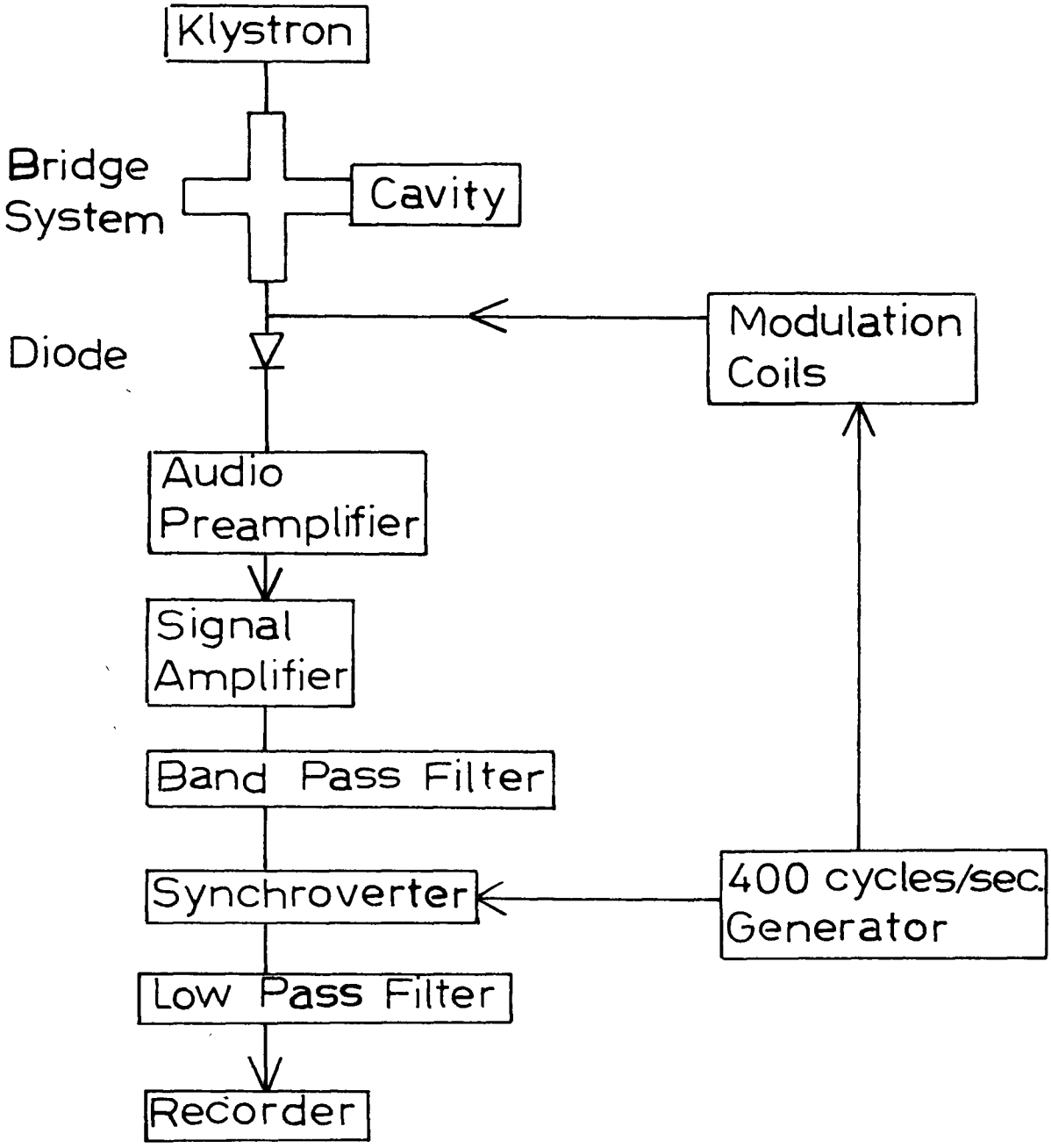

Figure 2. ESR Spectrometer

DETECTION SYSTEM.

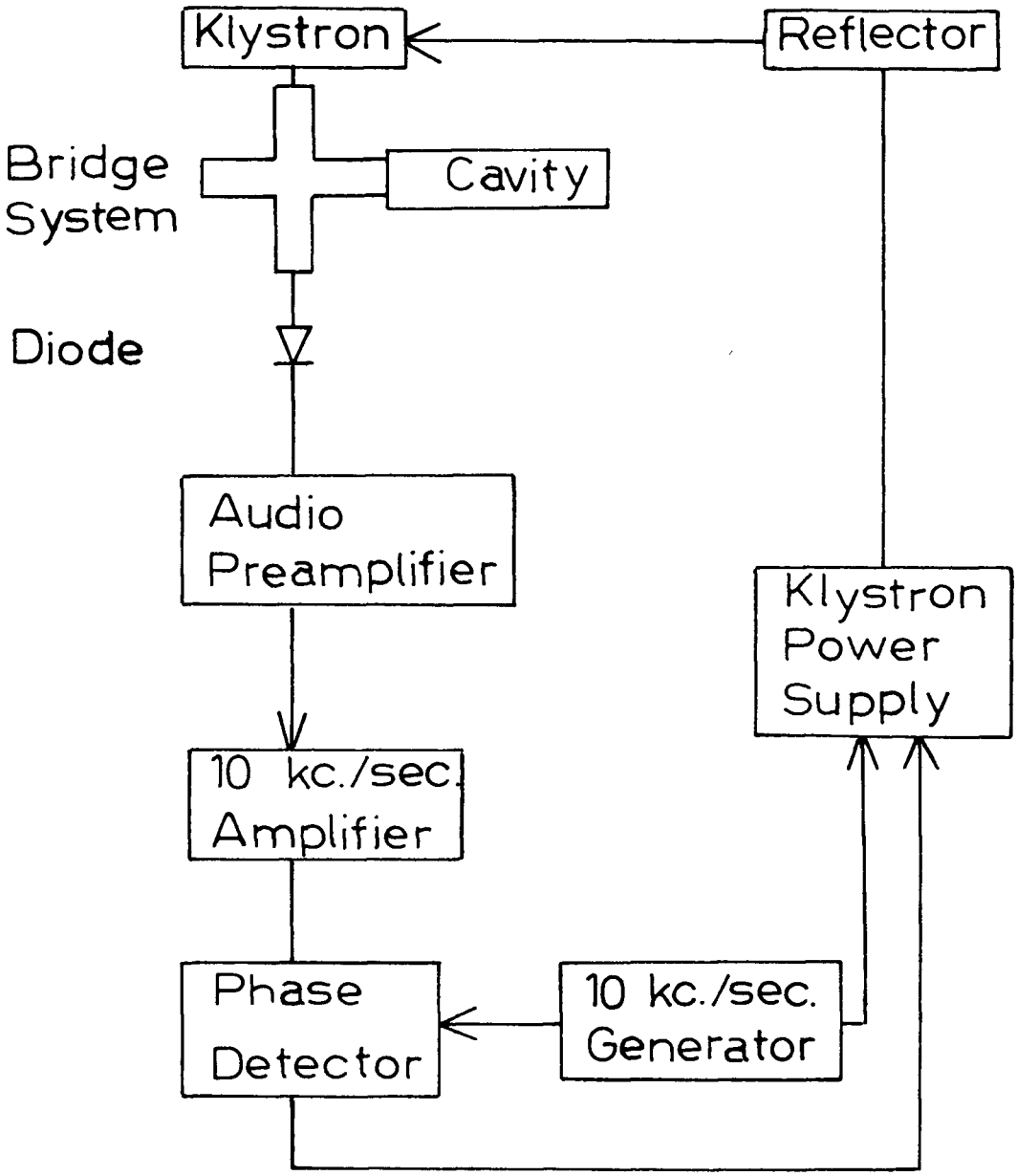

Figure 3. ESR Spectrometer

AUTOMATIC FREQUENCY CONTROL SYSTEM.

To Follow Page 10

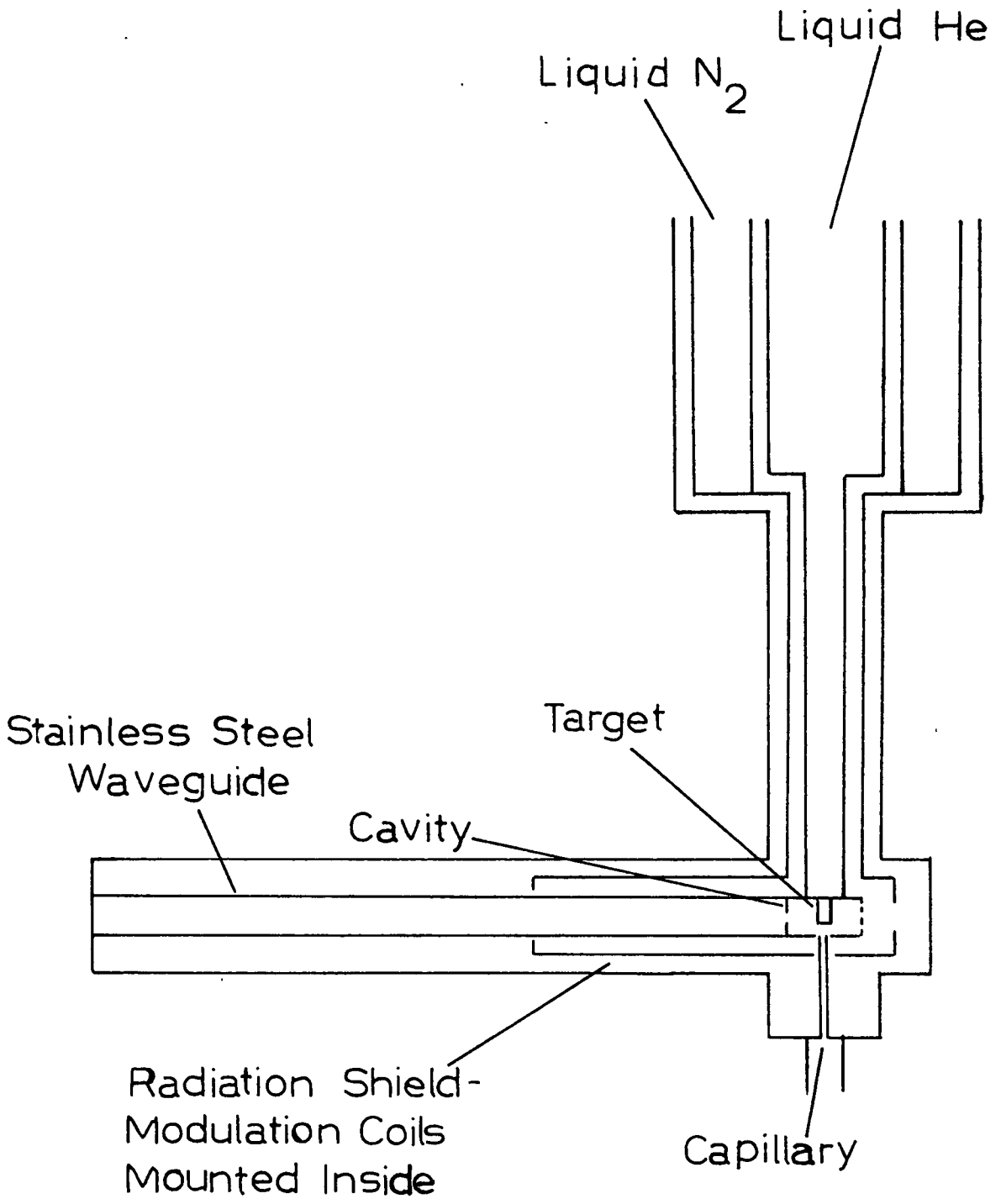

Figure 4. Liquid Helium Dewar.

evaporation of liquid helium due to entry of heat from external sources the cavity is connected to the external circuitry by a length of Type 304 stainless steel waveguide having a wall thickness of 0.01 inch. In the end wall of the cavity have been milled horizontal slots to allow irradiation of the sample in situ; the slots are 0.3 mm. wide and allow 50% of the incident radiation to enter the cavity. A hole in the bottom of the cavity permits insertion of a 1/16 in. outside diameter, 0.005 in. wall thickness stainless steel capillary through which the gaseous samples enter.

The following procedure was used to fill the dewar with liquid helium. At least one, and preferably three or more hours before the helium transfer the radiation shield was filled with liquid nitrogen. Then the liquid helium was siphoned from a storage dewar through a 3/16 in. outside diameter, 0.010 in. wall thickness stainless steel transfer tube enclosed in a vacuum jacket. The pressure on the liquid helium in the storage dewar was about $\frac{1}{2}$ pound/square inch above atmospheric during a transfer operation. Helium was liquefied in an adjacent Collins cryostat and gas evolved from the dewar was recovered for further use. Only by trial and error, and then from experience, could the operator decide when the dewar was full; indications of the dewar's being empty were such things as cessation of motion of the gas holder in the helium recovery system and an increase in the pressure in the vacuum system. It is hoped that a depth indicator using a superconducting tantalum wire, which is now

in the process of being constructed, will eliminate the guesswork in handling the lquid helium.

2-3 Production of Trapped Radicals

Vacuum techniques were used in handling samples. The following procedure was used in preparing gas mixtures. An evacuated, blackened three litre bulb was filled to an appropriate pressure (usually 1-5 mm. Hg) with a reagent gas (R) from which all air had been previously removed. Enough matrix gas (M) was then added to make up the desired mole ratio (M/R). If possible the sample was left to stand for a few days to allow mixing of the reagent and matrix. In many cases, however, this could not be done, and mixing was often promoted by warming the bottom of the bulb.

Two lamps were used to irradiate the samples. These were a General Electric A-H6 1000 watt mercury arc lamp and a General Electric H85A3/UV 85 watt mercury arc lamp; both were water cooled. Radiation from the lamp was focussed on the sapphire rod by a pair of quartz lenses set in a brass holder. The holder was constructed in such a way that the space between the lenses could be filled with water as a filter for any infrared radiation from the lamp. Filling with water was necessary when using the A-H6 lamp as otherwise the heat caused the liquid helium to boil off rather rapidly. Use of the water filter was not necessary for the H 85A3/UV lamp. Photolyses were carried out on the solid deposits using the full arc of the lamp; attempts to increase the efficiency of radical production by irradiating during deposition had little effect.

The course of action in an ESR experiment was as follows. After the appropriate lamp had been focussed on the sapphire rod and the dewar had been filled with liquid helium, the sample was passed from the bulb, through a flow regulator at a setting found by trial-and-error to give the most efficient rate of deposition, and thence onto the cooled sapphire rod via the stainless steel capillary. The sample was added either until the deposit could be seen (by looking through the waveguide) to be 1-2mm. thick (as in the case of experiments requiring photolysis) or until a fairly large signal was found (as in the experiments involving NO_2 and NF_2). When deposition was complete the lamp and microwave system were turned on, the frequency was measured, the microwave power was set at an appropriate level and the desired magnetic field region was scanned in search of an ESR signal.

The above was the general technique used in studying solid samples at 4.2^{o}K. Special treatments were often necessary, depending on the sample and experiment, and are described in the sections discussing the individual radicals.

CHAPTER THREE

THE METHYLENE RADICAL

3-1 Introduction

Throughout the past decade much interest has been centred about the methylene radical (CH_2). In the main the cause of such interest has been its two non-bonded electrons, and much work has been done to try to determine what happens to them in various conditions. Chiefly, however, most consideration has been given to the ground state and the decision as to whether it is a singlet or a triplet.

Theoretical predictions of the nature of various states of methylene have been as diverse as the number of papers involved, and have depended on the assumptions and treatments used and on the detail of the calculation. For example, Foster and B oys (17) used a variation method employing configuration interaction and predicted the ground state to be $^3B_1$, with an H-C-H bond angle of 129°. On the other hand Lennard-Jones (18), continuing some work of Mulliken (19), drew some correlation diagrams between isoelectronic species using molecular orbital theory and decided that the ground state of methylene should be $^1A_1$. Walsh (20) went further, drawing correlation diagrams for various species at different configurations, and although he decided that the ground state of methylene should be $^1A_1$ he pointed out that if the molecule were linear it would be $^3\Sigma_g^-$. Jordan and Longuet-Higgins (21), using a modified valence bond approach, and Pedley (22), from heat of formation considerations, have recently concluded that the ground state should be the

linear triplet. From these examples the diversity of the predictions is apparent.

Experimental findings seem more and more to favour the triplet as the ground state, although the evidence is indirect. In the photolysis of diazomethane in the presence of cis-2-butene Woodworth et al. (23) found stereospecific addition of methylene to the olefin to form cis-1,2-dimethylcyclopropane. Such stereospecificity would be expected, they point out, if the methylene were in a singlet state because conservation of spin would facilitate direct addition to the double bond. Addition of triplet methylene would have a diradical as an intermediate which would have a sufficient lifetime to permit loss of the stereospecificity as well as formation of 3-methyl-1-butene. Anet et al. (24) and Frey (25) did in fact find the latter phenomenon when the experiment was done in high pressures of inert gas and concluded that methylene, originally formed in the singlet state, had been degraded to a triplet ground state.

Attempts to trap methylene and perform ultraviolet and infrared studies on it have always yielded complicated spectra. Pimentel et al. (26)(27)(28) have made numerous infrared studies on the trapped photolysis products of diazomethane, and have based arguments concerning trapped methylene on the presence of absorptions whose disappearance on warmup coincided with the formation of ethylene. The most recent papers on such investigations, by Goldfarb and Pimentel (28) and by Robinson and McCarty (29), present complex and often conflicting results in infrared and ultraviolet studies of the phenomenon. The presence of

tautomers of diazomethane and extra photolysis products such as CH was probably the cause of the complication. Robinson and McCarty found some absorptions near 3200A° which they thought might have had as a lower state $^3\Sigma_g^-$ methylene, but in view of the evidence of Herzberg (30) this assignment appears doubtful. In all, previous work on trapped methylene has been highly inconclusive, for slight changes in experimental conditions seem to have far reaching effects.

In gas phase spectroscopic studies of the flash photolysis of diazomethane Herzberg et al. (30)(31) have found the most suggestive evidence for triplet methylene. The experiments, done in a high pressure of inert gas, revealed features in the vacuum ultraviolet which could be due to linear methylene (C-H bond distance 1.03Å). He also found features in the visible whose lower state was bent ($^1A_1$), but because a greater pressure of inert gas was required to produce the features in the ultraviolet he suggested that the lower state of this transition ($^3\Sigma_g^-$) was the ground state.

In the experiments described here an attempt was made to investigate the photolysis products of ketene (CH_2CO) and diazomethane (CH_2N_2) trapped at 4.2°K in solid argon and krypton. Ketene was tried first because of the dangerous properties of diazomethane even though earlier studies by Pimentel (32) of the photolysis in situ had revealed no decomposition, presumably because CH_2 and CO had recombined in the matrix cage. Diazomethane has the advantage that CH_2 does not react with the other photolysis product, N_2, and thus the cage has little effect, once

fragmentation has occurred. It was hoped that a triplet state for trapped methylene could be found by ESR. In view of the low temperature to be used and the number of collisions that methylene could undergo in the solid it is likely that any triplet state found would be the ground state.

The experiments are described in the following sections. An experiment involving the photolysis of CH_2N_2 in the presence of D_2O is also discussed.

3-2 Electron Spin Resonance of Triplet States, with particular consideration to methylene in a $^3\Sigma_g^-$ state.

A triplet state possesses two coupled unpaired electrons (i.e. $S=1$), and consequently should be detectable by ESR. The interactions described in equations (6) and (8) still exist, but there is a further one resulting from the spin-spin interaction of the electrons, which is often of very great magnitude and complicates matters considerably. Data on ESR of triplet states are rather sparse, although some do exist (33) - (37).

For two unpaired electrons in a triplet state contribution from spin-spin interaction can be adequately described by the following Hamiltonian:

$$\mathcal{H}_{ss} = g^2\beta^2\left\{\frac{\bar{S}_1\cdot\bar{S}_2}{r^3} - \frac{3(\bar{S}_1\cdot\bar{r})(\bar{r}\cdot\bar{S}_2)}{r^5}\right\} \qquad (19)$$

where $\bar{S}_1$, $\bar{S}_2$, are spin operators of the individual electrons and $\bar{r}$ is the interelectronic vector of length r. (Because the spin part of the triplet wave function is symmetric the spatial part must be antisymmetric, so that always $r\neq 0$ and the contact term in $\mathcal{H}_{ss}$ vanishes). If now equation (19) is expanded into

components in Cartesian coordinates $\mathcal{H}_{ss}$ becomes, after some algebraic manipulations:

$$\mathcal{H}_{ss} = -g^2\beta^2\left[\frac{3xy}{r^5}\left(S_{1x}S_{2y}+S_{1y}S_{2x}\right)+\frac{3yz}{r^5}\left(S_{1y}S_{2z}+S_{1z}S_{2y}\right)\right.$$
$$+\frac{3zx}{r^5}\left(S_{1z}S_{2x}+S_{1x}S_{2z}\right)+\frac{3}{2}\frac{x^2-y^2}{r^5}\left(S_{1x}S_{2x}-S_{1y}S_{2y}\right) \quad (20)$$
$$\left.+\frac{1}{2}\frac{3z^2-r^2}{r^5}\left(3S_{1z}S_{2z}-\bar{S}_1\cdot\bar{S}_2\right)\right]$$

Let us now consider CH_2 in the axially symmetric linear $^3\Sigma_g^-$ state. In this state the spin wave function is a triplet, the orbital angular momentum about the molecular (z) axis is zero, and the spatial wave function is symmetric to inversion through the centre of symmetry but antisymmetric to reflection in any plane running through the z-axis. In this case any integrations of $\mathcal{H}_{ss}$ over the spatial part of the wave function cause the first four terms to vanish leaving only

$$\mathcal{H}_{ss} = -g^2\beta^2\left(\frac{3z^2-r^2}{2r^5}\right)\left(3S_{1z}S_{2z}-\bar{S}_1\cdot\bar{S}_2\right) \quad (21)$$

One can take as zero order spin functions of the triplet state:

$$\begin{aligned}|M_S=1\rangle &= \alpha_1\alpha_2\\ |M_S=0\rangle &= \frac{1}{\sqrt{2}}\left(\alpha_1\beta_2+\beta_1\alpha_2\right)\\ |M_S=-1\rangle &= \beta_1\beta_2\end{aligned} \quad (22)$$

where α and β mean spins parallel and antiparallel to the molecular axis and subscripts 1 and 2 mean electrons 1 and 2. The states [eq. (22)] are eigenfunctions of $S^2=\bar{S}\cdot\bar{S}$, $\bar{S}$ being the total spin operator. Now $\bar{S}=\bar{S}_1+\bar{S}_2$ and its z-component $S_z=S_{1z}+S_{2z}$,

whence:

$$\bar{S}\cdot\bar{S} = S^2 = S_1^2 + S_2^2 + 2\bar{S}_1\cdot\bar{S}_2$$
$$S_z^2 = S_{1z}^2 + S_{2z}^2 + 2S_{1z}S_{2z} \qquad (23)$$

and: $$\mathcal{H}_{ss} = -g^2\beta^2\left[\frac{3z^2-r^2}{4r^5}\left(3S_z^2 - 3S_{1z}^2 - 3S_{2z}^2 - S^2 + S_1^2 + S_2^2\right)\right] \qquad (24)$$

Also,

$$\begin{aligned} S_1^2|M_s\rangle &= \tfrac{3}{4}|M_s\rangle \\ S_2^2|M_s\rangle &= \tfrac{3}{4}|M_s\rangle \\ S_{1z}^2|M_s\rangle &= \tfrac{1}{4}|M_s\rangle \\ S_{2z}^2|M_s\rangle &= \tfrac{1}{4}|M_s\rangle \end{aligned} \qquad (25)$$

so that:

$$\mathcal{H}_{ss}|M_s\rangle = -g^2\beta^2\left[\frac{3z^2-r^2}{4r^5}\left(3S_z^2 - S^2\right)\right]|M_s\rangle \qquad (26)$$

One can represent the spatial part of the zero-order wave function by $\psi(\bar{r}_1,\bar{r}_2)$, where $\bar{r}_1, \bar{r}_2$ are the spatial coordinates of the two electrons, so that the overall zero-order wave function is:

$$\Psi = \psi(\bar{r}_1,\bar{r}_2)|M_s\rangle \qquad (27)$$

The overall Hamiltonian, ignoring hyperfine and nuclear Zeeman terms, which are small compared to the electron Zeeman term and $\mathcal{H}_{ss}$, becomes:

$$\mathcal{H} = g\beta\bar{H}\cdot\bar{S} - g^2\beta^2\left[\frac{3z^2-r^2}{4r^5}\left(3S_z^2 - S^2\right)\right] \qquad (28)$$

B ecause of the axial symmetry one can consider components of $\bar{H}$ perpendicular to the molecular axis as being along the x-axis.

In this case the matrix for the Zeeman term is

$$g\beta\bar{H}\cdot\bar{S} = g\beta \begin{pmatrix} H_z & H_x/\sqrt{2} & 0 \\ H_x/\sqrt{2} & 0 & H_x/\sqrt{2} \\ 0 & H_x/\sqrt{2} & -H_z \end{pmatrix} \qquad (29)$$

For $\mathcal{H}_{ss}$ it is

$$-g^2\beta^2\left(\frac{3z^2-r^2}{4r^5}\right)\left(3S_z^2-S^2\right) = T\begin{pmatrix} 1 & 0 & 0 \\ 0 & -2 & 0 \\ 0 & 0 & 1 \end{pmatrix} \qquad (30)$$

where T is the integral $\left\langle \psi(\bar{r}_1,\bar{r}_2)\left|\frac{-g^2\beta^2(3z^2-r^2)}{4r^5}\right|\psi(\bar{r}_1,\bar{r}_2)\right\rangle$

The overall Hamiltonian is then:

$$\mathcal{H} = \begin{pmatrix} T+g\beta H_z & g\beta H_x/\sqrt{2} & 0 \\ g\beta H_x/\sqrt{2} & -2T & g\beta H_x/\sqrt{2} \\ 0 & g\beta H_x/\sqrt{2} & T-g\beta H_z \end{pmatrix} \qquad (31)$$

At zero field, i.e. when $H_x = H_z = 0$, equation (31) becomes:

$$\mathcal{H} = \begin{pmatrix} T & 0 & 0 \\ 0 & -2T & 0 \\ 0 & 0 & T \end{pmatrix} \qquad (32)$$

The states $|0\rangle, |1\rangle, |-1\rangle$ are thus eigenstates of $\mathcal{H}$ under these conditions, the first having energy $-2T$ and the latter two being degenerate at an energy T. The separation, $3T$, called the zero-field splitting, is the cause of much of the difficulty in detecting triplet states by ESR. It depends solely on the spatial part of the wave function and can be very large. For

oxygen molecules (35)(38) it has been found to be 92,200 mc./sec., and Coope (39) has estimated that for linear methylene it is at least 32,890 mc./sec. These energies are very much greater than those of 9500 mc./sec. used in most X-band ESR spectrometers, and may necessitate use of special techniques. Indeed, ESR studies of O_2 in clathrates required use of a special cavity and pulsed magnetic fields (35).

If a magnetic field is oriented along the z-axis the Hamiltonian matrix becomes

$$\mathcal{H} = \begin{pmatrix} T + g\beta H_0 & 0 & 0 \\ 0 & -2T & 0 \\ 0 & 0 & T - g\beta H_0 \end{pmatrix} \qquad (33)$$

$|1\rangle, |0\rangle, |-1\rangle$ are again eigenstates of $\mathcal{H}$, this time at energies of $T+g\beta H_0, -2T, T+g\beta H_0$. These are shown diagrammatically in Figure 5 for a zero field splitting of 33,000 mc./sec. When a radio frequency magnetic field is oriented perpendicular to $\bar{H}$ (as in the present case), magnetic dipole transitions occur according to the selection rule $\Delta M_s = \pm 1$ at energies of $|3T \pm g\beta H_0|$. The $\Delta M_s = \pm 2$ transition is forbidden. It must be remembered that in most ESR experiments the frequency of the microwave cavity (i.e. the energy transition studied) is kept constant and the magnitude of the zero field splitting may be such that some transitions, though allowed, may not be observable in a given experimental situation.

If now the magnetic field is applied perpendicular to the molecular axis (i.e. along the x-axis) the Hamiltonian matrix becomes:

To Follow Page 21

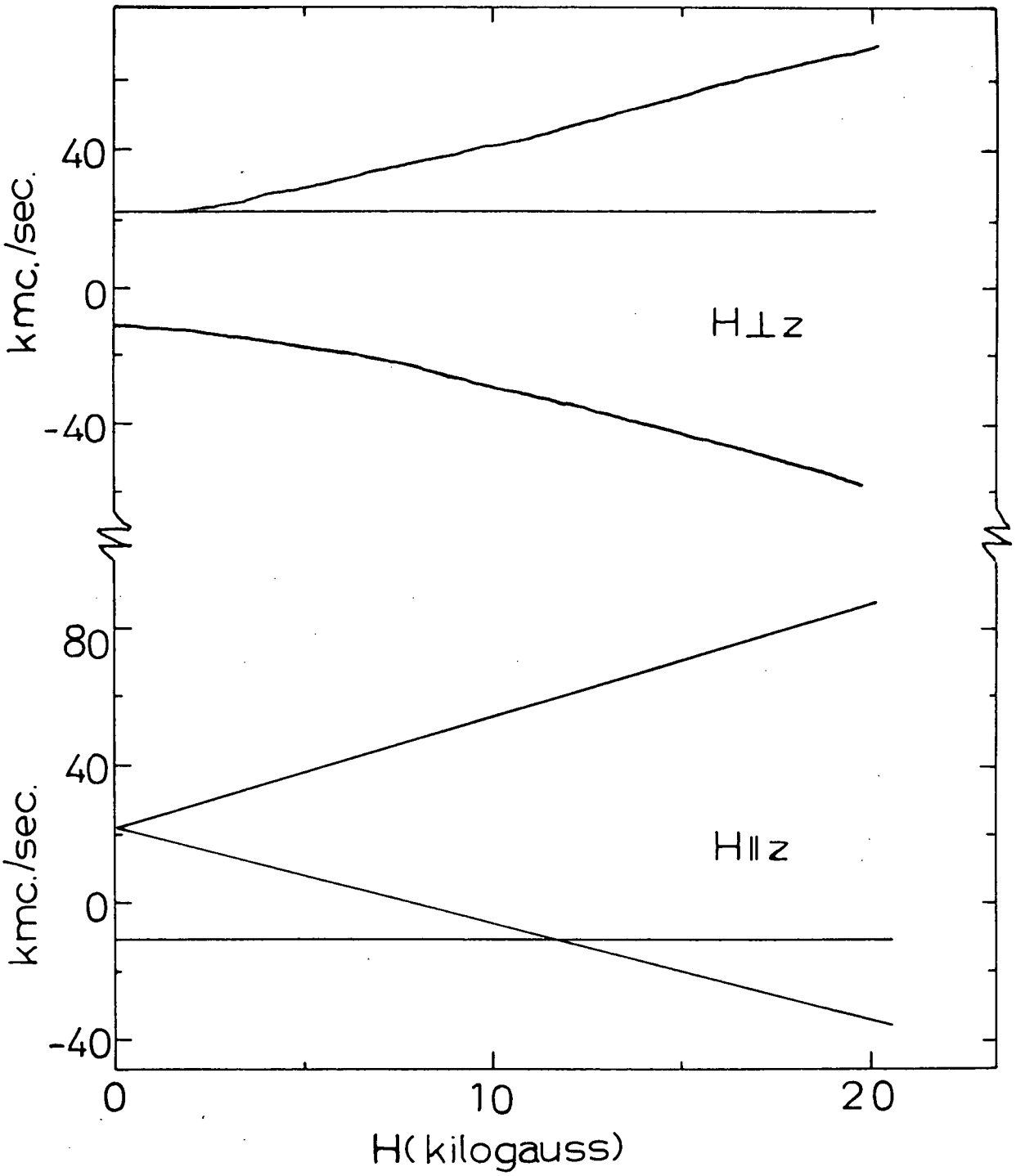

Figure 5. Energy Level Diagrams for the Spin Hamiltonian of Equation (28) for a Triplet State with a Zero Field Splitting of 33 kmc./sec.

$$\mathcal{H} = \begin{pmatrix} T & g\beta H_0/\sqrt{2} & 0 \\ g\beta H_0/\sqrt{2} & -2T & g\beta H_0/\sqrt{2} \\ 0 & g\beta H_0/\sqrt{2} & T \end{pmatrix} \qquad (34)$$

The eigenvalues and their corresponding eigenfunctions are given in Table I below:

TABLE I

Eigenvalues and Eigenfunctions of a Triplet State of a Linear Molecule when a Magnetic Field is Oriented Perpendicular to the Symmetry Axis.

Eigenvalue	Eigenfunction
T	$1/\sqrt{2}\ (\|-1\rangle - \|1\rangle)$
$\frac{-T \pm \sqrt{9T^2 + 4g^2\beta^2H_0^2}}{2} = \frac{-T \pm \delta}{2}$	$\left(\frac{\delta \pm 3T}{4\delta}\right)^{1/2}\|1\rangle + \left(\frac{\delta \mp 3T}{2\delta}\right)^{1/2}\|0\rangle + \left(\frac{\delta \pm 3T}{4\delta}\right)^{1/2}\|-1\rangle$

The magnetic dipole transitions are now allowed between all three eignenstates, and occur at energies of $\left|\frac{3T \pm \sqrt{9T^2 + 4g^2\beta^2H_0^2}}{2}\right|$ and $\sqrt{9T^2 + 4g^2\beta^2H_0^2}$. Observation of transitions is subject to the same experimental restrictions as for the case of $\bar{H} \parallel z$. A diagram of the energy levels is given in Figure 5.

In the case of the magnetic field being neither parallel nor perpendicular to the molecular axis the eigenstates become further combinations of the basis states. The energy levels change with the field, as well as the angle between the field and the molecular axis, in a complicated fashion. As a result

the fields at which the transitions may occur also have a complex dependence on the angle.

The experiments to be described here concern attempts to trap methylene in a polycrystalline matrix of solid inert gas. A number of possible situations may arise; the first is that the radicals are held rigidly in the matrix. In this case one obtains all orientations of the radicals with respect to the field. Transitions occur over a continuous range of fields about $\frac{h\nu}{g\beta}$, the magnitude of the range being dependent on the zero field splitting. It is very likely that this broadening would prevent detection of any transition at fields close to that corresponding to g = 2. In the field region of g = 4. detection is more likely, but could occur only if $3T < \sim \frac{2}{3} h\nu_0$ (ν_0 = cavity frequency) (34). In view of Coope's predicted value for $3T > 32,890$ mc./sec. and the frequency of 9500 mc./sec. used in the experiments it is unlikely that such a condition would be met. The result is that if the radicals are held rigidly it is most improbable that they would be detectable.

If the radicals are isotropically rotating at frequencies very much greater than $T/\hbar$ then a similar situation to that found for the anisotropic part of the hf interaction would occur, namely that the zero field splitting would average to zero. In this case transitions occurring in the field region of g = 2 would be detectable.

For hindered rotation the situation becomes much more complicated. For the case of O_2 trapped in quinol clathrates, a situation rather similar to that found in the present

experiments, the zero field splitting is merely reduced (38). It has been suggested that there is a hindrance potential to rotation of the form $V_0 (1 - \cos 2\xi)$, where ξ is the angle between the molecular (z) axis and the direction of minimum potential in the cage (z'). This reduces the zero field splitting to $3T' = 3T\left[\frac{3}{2}\langle\cos^2\xi\rangle_{av.} - \frac{1}{2}\right]$ and transforms the Hamiltonian $\mathcal{H}$ to

$$\mathcal{H} = g\beta\bar{H}\cdot\bar{S} + 3T'\left[S_{z'}^2 - \tfrac{1}{3}S(S+1)\right] \qquad (35)$$

Quantization of $\bar{S}$ is now in the direction of z'. In this case the radicals would not be detectable at g = 2.

3-3 Experimental Methods

A. Ketene

The ketene used was kindly supplied by Dr. G. B. Porter, who had prepared it by pyrolysing acetic anhydride. As ketene boils at - 56°C and reacts with water to give poisonous acetic acid vapour it was necessary to keep it in liquid nitrogen. Its purity was checked in a mass spectrometer, and the small amounts of ethylene and carbon monoxide found in this way were removed by freezing and warming the sample between 77 and 195°K. Gas mixtures of ketene and Matheson Research Grade argon were prepared at matrix ratios (M/R) of 100 and 300. The general deposition technique described earlier was modified by bypassing the brass flow regulator to reduce any metal catalysed polymerization of the ketene (although the sample had nevertheless to pass through the stainless steel capillary into the cavity). The General Electric A-H6 lamp was used to irradiate the solid sample. Magnetic fields in the region of g = 2 and g = 4 were scanned in searching for methylene resonance; the microwave power varied

between five and 100 milliwatts.

B. Diazomethane

Diazomethane was prepared in the laboratory before each attempt to produce methylene. Since diazomethane is both highly toxic and explosive it was necessary to carry out the preparation in a fume cupboard and to wear protective clothing while handling the compound.

Two methods were used for the sample preparations. The one used for all the experiments involving the search for methylene used the synthesis method of de Boer and Backer (40) for gaseous diazomethane. The apparatus is shown schematically in Figure 6. The procedure was as follows. A solution of 3 gm. KOH in 3 ml. water and 25 ml. 2-(2-ethoxyethoxy) ethanol was warmed with a heating pad to 50-60 ^{o}C in the specially modified 125 ml. long stemmed flask. To this was added dropwise a solution of 6.5 gm. N-methyl N-nitroso p-toluenesulfonamide ("Diazald" from Aldrich Chemical Company) in 10 ml. anisole, and the diazomethane produced in the ensuing reaction was extracted by bubbling inert gas (argon or helium) gently through the mixture. The gases were cooled in a condenser, passed through a trap containing KOH pellets to remove any water, cooled further in a trap at 195 ^{o}K (CO_2- acetone), and the diazomethane was finally condensed in a trap at 77 ^{o}K (liquid N_2). The system of traps was closed to the atmosphere and any non-condensable gas was pumped off. The trap containing diazomethane was warmed to 195 ^{o}K, and the compound distilled to a third trap at 77 ^{o}K. Finally the third trap was warmed to 195 ^{o}K and a middle fraction

of the gas evaporating from this was collected in a bulb and transported to the vacuum system connected to the ESR spectrometer. The purity of the diazomethane was checked in a Perkin-Elmer 21 Infrared Spectrometer and although peaks were observed at 2800-2900 $cm.^{-1}$ (the aliphatic C-H stretch region; the peaks may have been due to an impurity or possibly a cyclic CH_2N_2 dimer) all others were those reported for diazomethane (41) and the sample was used. (A further middle fraction of the sample obtained as above failed to reduce the relative intensity of the peak at 2800-2900 $cm.^{-1}$.) Samples for ESR study were prepared in the usual way at matrix ratios from 100 to 300 using Matheson Research Grade argon and krypton as matrices. Because diazomethane decomposes on long standing the samples had to be used after only one or two hours mixing. The samples were deposited in the usual way, and the A-H6 lamp was used for the irradiation. The search for an ESR signal followed the same procedure as for ketene.

In the experiment involving D_2O a slight modification of the method of Dr. J. A. Bell (42) was used for the diazomethane synthesis. It was adopted in an attempt to reduce the number of possible impurities in the sample, for it eliminated the necessity of heating and using a carrier gas and permitted the use of a mercury diffusion pump, which the previous apparatus did not do. The apparatus is shown in Figure 7 and the method used was as follows. Using the Y-shaped tube shown in Figure 7 dry N-methyl N-nitroso p-toluene sulfonamide was added <u>in vacuo</u> to a solution of KOH in ethylene glycol which had been previously degassed and cooled to $0^{\circ}C$ to prevent decomposition of any

diazomethane formed. (It was necessary to prepare the KOH solution by dissolving the hydroxide slowly in ethylene glycol at room temperature; heating caused the solution to turn yellow with a simultaneous increase in viscosity, possibly due to the formation of a polymer.) The vapours produced were extracted from the generating system by slight pumping, passed through a tube containing glass wool to catch any droplets which might have bumped out of the solution, and condensed in a trap at 77°K. Any ethylene condensing in the trap was removed by a flash distillation and the diazomethane remaining was condensed in a bulb and transported to the other bulb as before. The whole procedure was carried out in the dark in order to minimize photolysis of diazomethane.

In the preparation of the gas mixture the three litre bulb was filled with the diazomethane sample to 4 mm.Hg and the pressure was increased to 15 mm. Hg by addition of D_2O. (All air had been previously removed from the D_2O by freezing to 195°K, pumping and then warming with the pump off. The procedure was repeated six times.) Finally argon, the matrix gas, was added to bring the total pressure to just over 30 cm. Hg. After the gases had been mixing at room temperature for about an hour the sample was deposited on the sapphire needle at 4.2°K in the usual way and the solid was irradiated with the full arc of the A-H6 lamp. The field region of g = 2 was searched for an ESR signal using a microwave power level of 2-5 mw.

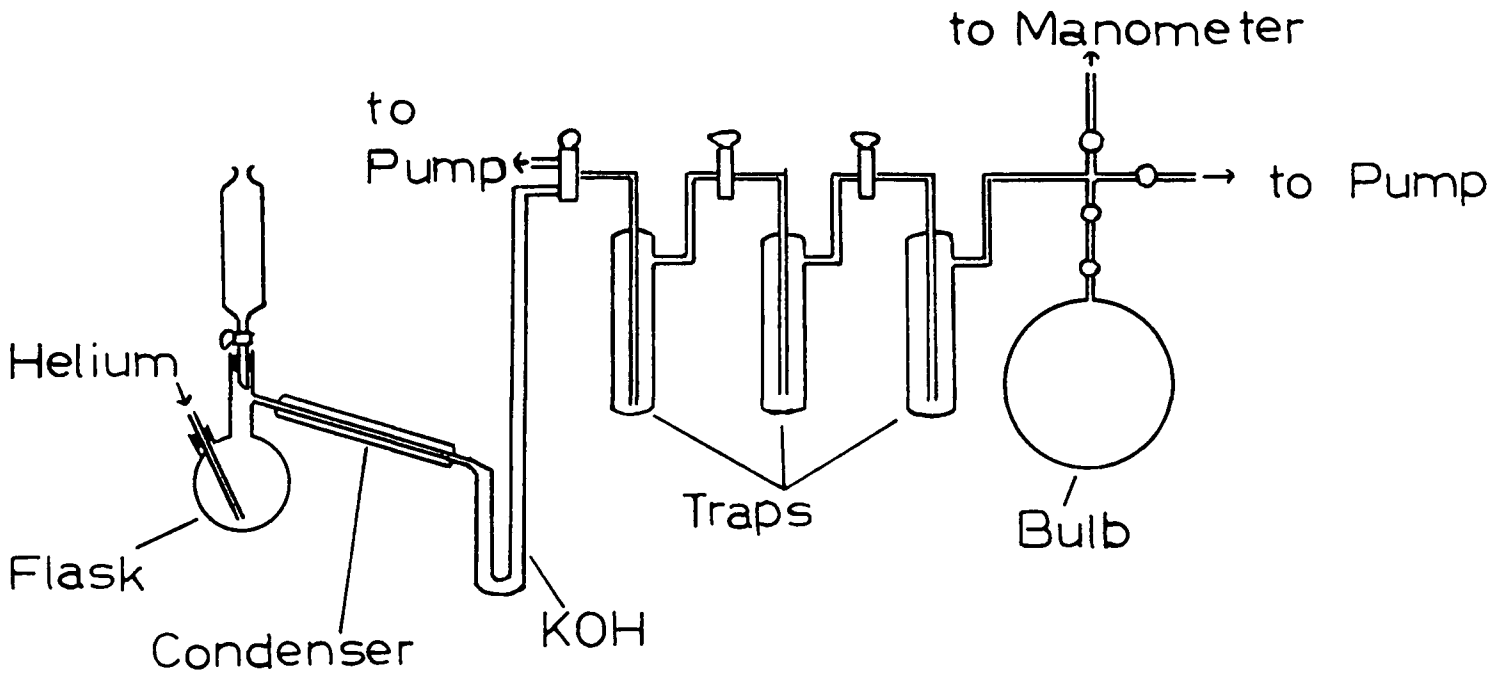

Figure 6. Vacuum System for CH_2N_2 Preparation
(Method of de Boer and Backer).

To Follow Page 27

To Follow Page 27

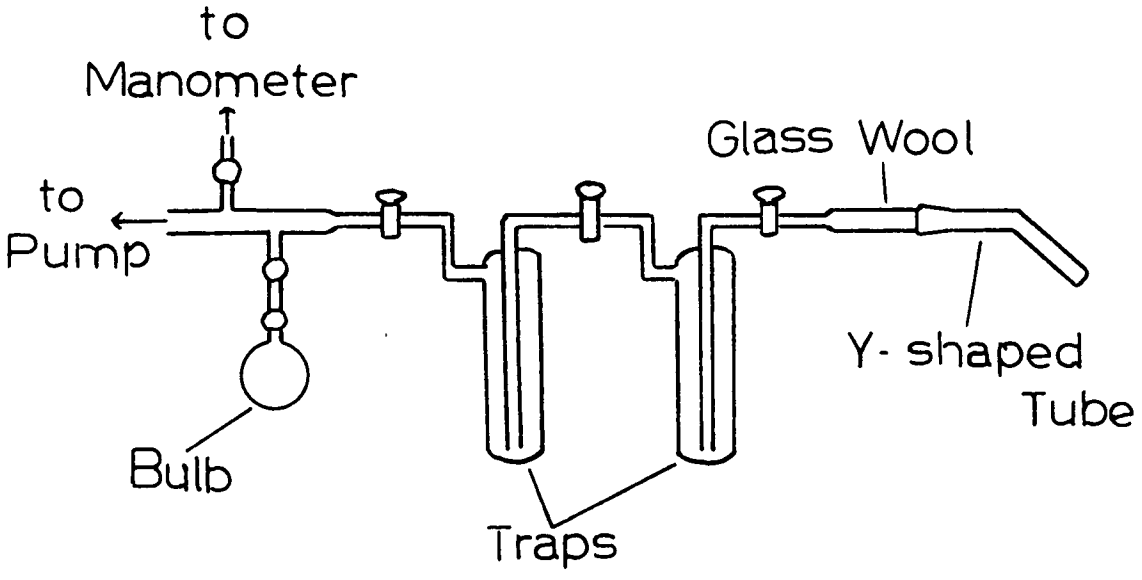

Figure 7(a). Vacuum System for CH_2N_2 Preparation (Method of Bell).

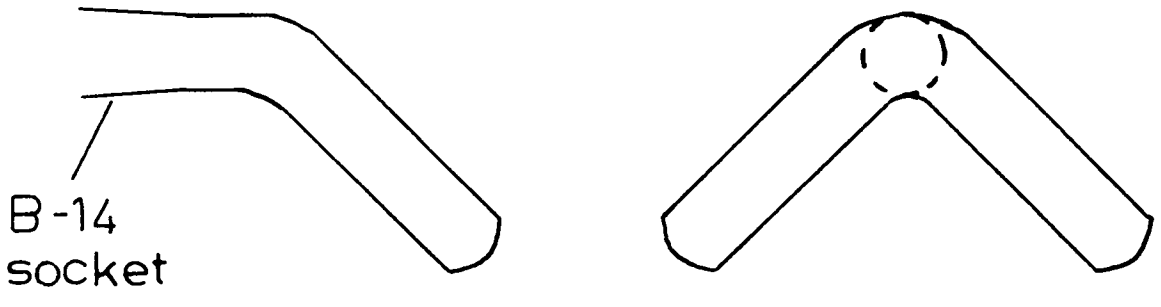

Side View End View

Figure 7(b). Y- shaped Tube.

3-4 Results and Discussion

The results of the experiments involving the search for methylene are shown in Table II. The most obvious facts in the table are that no definite, reproducible signal attributable to methylene was found, and on numerous occasions methyl radicals were obtained. Furthermore, when the wide signal was obtained it was almost always in conjunction with that of the methyl radical (except in run 6, and in this run difficulties were encountered with the spectrometer). Also a suggestion of a signal at g = 4 was found only once (run 8) and this was detected only at extreme settings of field modulation, amplitude and signal level. It should be noticed also that the methyl signal and the wide one were produced from both ketene and diazomethane when the matrix ratio was 100, but not when it was 300. It seems most improbable that trapping of methylene radicals would have been less likely at M/R = 300 than at M/R = 100 and it must appear that the methyl radicals and the radicals causing the wide signal were produced in the same process. If this were the case then the ESR absorption of trapped methylene radicals was probably not detected.

Methyl radicals could have been prepared either by the photolysis of an impurity or by the abstraction of hydrogen atoms from something by methylene. Photolysis of methyl iodide is a well known example of the first type of reaction, while the reaction of methylene with propane (43) is an example of the second. It is by no means impossible that abstraction to produce the methyl radical and a large rigidly trapped radical actually occurred, and the fact that the radicals were observed only at the low matrix ratio, when something other than inert gas was more

TABLE II

The Results of the Experiments Involving the Search for Methylene.

Experiment	Sample	Matrix Ratio	Result
1	CH_2CO/Ar	300	nil
2	CH_2CO/Ar	300	slight indication of signal
3	CH_2CO/Ar	300	nil
4	CH_2CO/Ar	300	nil
5	CH_2N_2/Ar	100*	at g = 2 wide signal; CH_3 present
6	CH_2N_2/Ar	100	at g = 2 possible wide signal
7	CH_2CO/Ar	100	CH_3 present
8	CH_2N_2/Ar	100	at g = 2 strong wide signal; CH_3 present at g = 4 possible wide signal
9	CH_2N_2/Ar	100	at g = 2 weak wide signal; CH_3 present
10	CH_2N_2/Ar	-	at g = 2 weak wide signal; CH_3 present
11	CH_2N_2/Kr	100-300	nil#
12	CH_2N_2/Kr	200-300	nothing definite

* Diethyl ether was present in the sample.

\# A pyrex filter was used.

accessible to methylene, adds weight to the argument.

To test the abstraction hypothesis the experiment involving CH_2N_2 in the presence of D_2O was carried out. Although the ease of abstraction of hydrogen atoms from water would be less than that from hydrocarbons because of the greater bond energy in water, it was hoped that the radical CH_2D could be prepared. D_2O was chosen, however, because it is easily obtained and because any OD generated in an abstraction would probably not be detected because its g-factor is not 2. (However, in ice, a polar matrix, the orbital angular momentum may be quenched and the radical detected (44) in this field region. The separation of the lines in OD is about 6 gauss.) Possible photolysis of D_2O was discounted because the energy of the radiation was too low to break the OD bond.

A spectrum was obtained in the experiment and is shown in Figure 9. The four line signal of methyl was very prominent, but there were some other absorptions interspersed, the most noticeable being a triplet between the two most intense methyl lines. Between the outer methyl lines there were further weak absorptions. All the lines were very narrow, suggesting that the radicals producing them showed some degree of rotational freedom in the matrix. Now the ESR spectrum of CH_2D would probably show three sets of triplets symmetrically arranged about the free spin g-value with the centres of each triplet about 24 gauss apart and each line in the triplet 3.7 gauss apart. The expected intensity ratio of the lines would be 1:1:1:2:2:2:1:1:1. The lines found in the centre triplet surrounded a g-factor of $2.0015 \pm .0002$ and were 4.2 ± 0.3 gauss apart, very nearly the separation expected (but very much less

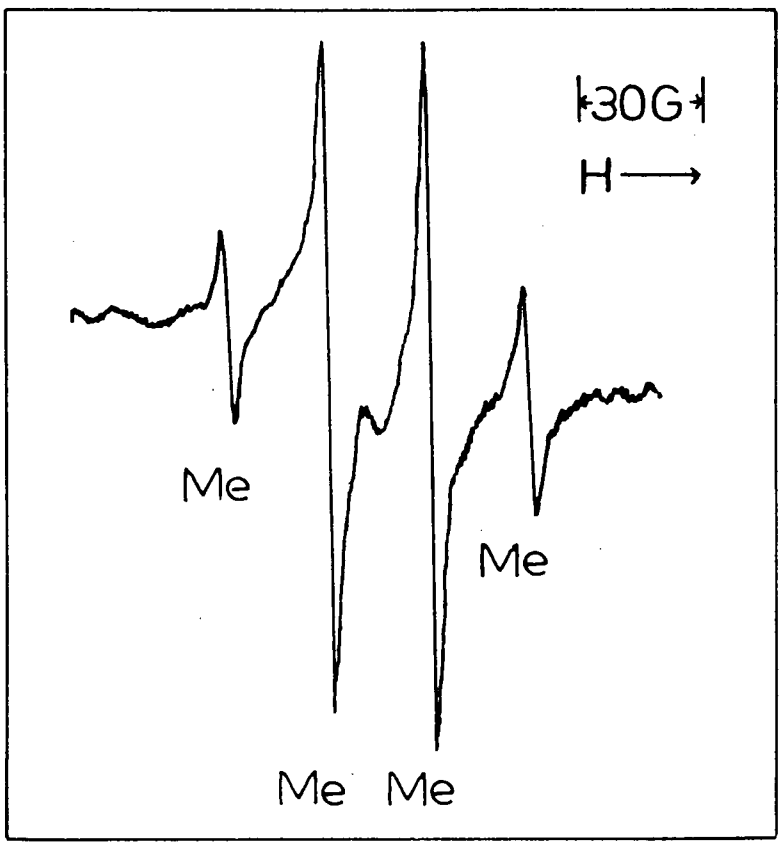

Figure 8. A Typical ESR Spectrum from the Photolysis of CH_2N_2 in Argon at 4.2°K. The lines marked by Me are due to the CH_3 radical. G denotes gauss.

To Follow Page 30

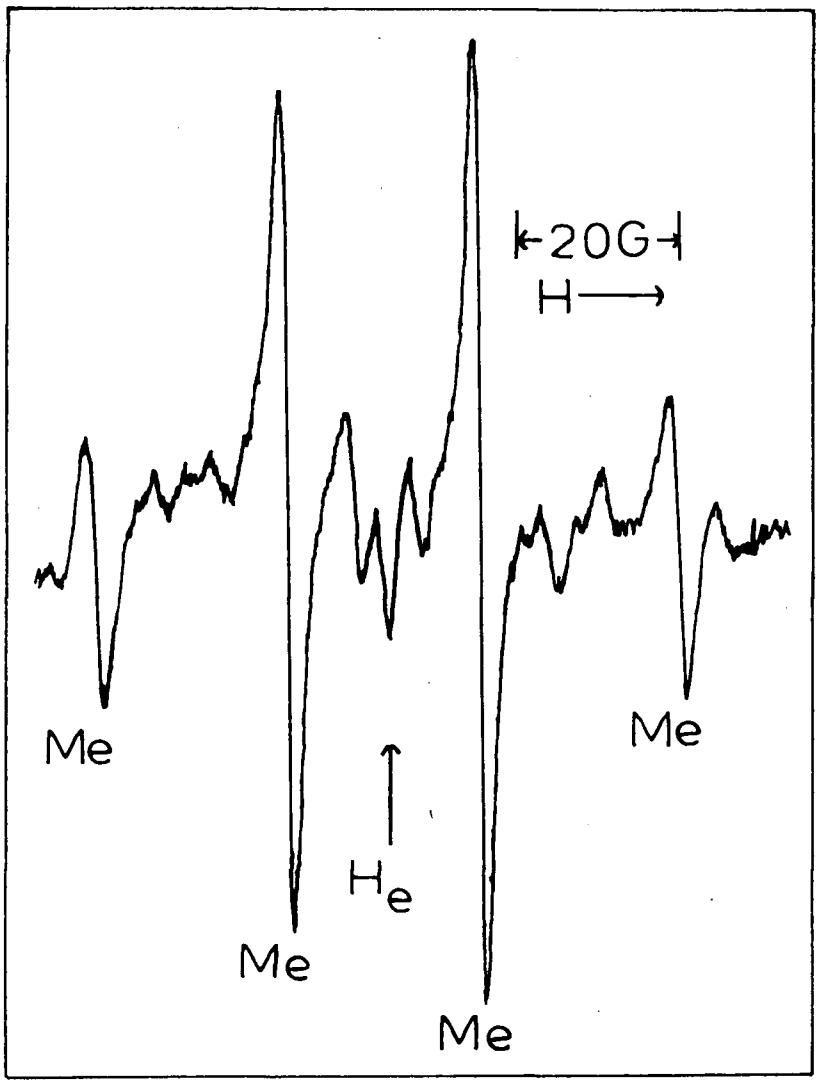

Figure 9. ESR Spectrum from the Photolysis of CH_2N_2 in the Presence of D_2O. Lines marked by Me are due to the CH_3 radical. G denotes gauss. H_e is the magnetic field where g=2.0023.

than 6 gauss found for OD). The strange shape of the triplet may well have been caused by its being superimposed on the broad resonance found earlier in conjunction with the production of CH_3 radicals from diazomethane. Although it was difficult to identify any triplets amongst the outer peaks the low signal-to-noise level may have been obscuring them. Thus the production of CH_2D was suggested; time considerations prevented further pursuit of the problem.

The appearance of the spectrum of ordinary methyl in the water experiment was hardly surprising. The matrix ratio $Ar + D_2O/CH_2N_2$ was only 80, ideal conditions according to the previous experiments for production of methyl radicals. The great intensity of the methyl spectrum compared with that of the other lines could be attributed to greater ease of abstraction of H from CH than of D from OD. In all the experiment added impetus to the suggestion that the methyl radicals found earlier arose through an abstraction mechanism.

In considering the problem of the non appearance of a signal due to methylene a very obvious question comes to mind, viz.,were any methylene radicals trapped? The abstraction mechanism just discussed, if correct, suggests that they were produced, although it does not say for how long. It is possible that methylene radicals may have decomposed or that other products may have been obtained, a situation suggested by the data of Robinson and McCarty (29). Pimentel (28) however, did manage to trap a precursor for ethylene, which was almost certainly methylene, using radiation of energies similar to

those used here. It is inconceivable that methylene could be produced at a matrix ratio of 100 but not one of 300, and one thus suggests that it was indeed trapped and the reason for the lack of an ESR signal must be found elsewhere.

Of course, if the trapped radicals were not in a triplet state no signal could have been obtained. In view of the results of Herzberg (30) this is an unlikely situation, for as was pointed out earlier any trapped radicals were probably in the ground state and the ground state is almost certainly the triplet ($^3\Sigma_g^-$). Furthermore the observation of abstraction may indicate the presence of a triplet, for Richardson et al. (45) have suggested that singlet methylene may show random insertion into carbon hydrogen bonds whereas the triplet may show abstraction. Trapped triplet methylene radicals were thus very probable.

If any trapped methylene radicals were held rigidly in the matrix, then they would have been undetectable in these experiments because of the high zero-field splitting. Again we have an unlikely situation, for the ESR spectrum of methyl radicals, which are of comparable size, indicates rotation of this radical in the matrix and methylene should do likewise (although rotation via the tunnel effect is much more likely for methyl than for methylene), Now at $4.2^{\circ}K$ freely rotating methylene should be in the ground ($J=0$) and first excited ($J=1$) rotational states, and the frequencies of rotation should be zero and $4.8 \times 10^{+11}$ sec.$^{-1}$ respectively. Since the zero-field splitting is between 3.3×10^{10} and about 7×10^{10} sec.$^{-1}$ then for the radicals in the $J=1$ state it is very possible that the effect of the electron spin-spin

interaction could be averaged to zero and ESR transitions could be observable at g = 2. The lack of an observed signal suggests that this was not the case.

Most likely the situation was similar to that of oxygen in a quinol clathrate (35), namely that the radicals were undergoing hindered rotation and that in the cage there was a direction of minimum potential energy. As will be discussed later in the thesis methyl radicals in an argon matrix probably undergo hindered rotation, and the situation was probably similar for methylene. The zero field splitting would have been merely reduced, and as the cages were randomly oriented in the polycrystalline matrix the effect in the experiments would have been the same as for rigidly trapped radicals.

CHAPTER FOUR

POPULATIONS OF ROTATIONAL STATES OF THE METHYL RADICAL

4-1 Introduction.

In the ESR spectrum of the NH_2 radical one would expect at first glance that the intensities of the hf peaks due to the hydrogen nuclei should be in the ratio 1:2:1, with three due to nitrogen of intensity ratio 1:1:1 superimposed on each. Instead Foner et al. (3) found all nine lines to be of approximately equal intensity, and McConnell (47) proposed an explanation based on the premises that the radicals were rotating freely and that the statistical distribution of the radicals in rotational states corresponded to thermal equilibrium. Using data for ND_2 Jen (48) carried the argument further and decided from the peak intensities that both ND_2 and NH_2 were undergoing hindered rotation in the matrix.

In the ESR spectrum of the $CH_3C(COOH)_2$ radical Heller (49) found four peaks due to hf interaction of the electron and the methyl protons, whose intensity ratio was 1:3:3:1 at room temperature but decreased to 1:1.45:1.45:1 at 4.2°K. From considerations similar to those of McConnell he decided that the methyl group underwent nearly free rotation about the C-C bond at 4.2°K.

The ESR spectrum of methyl radicals is well known (5). It contains four sharp lines, centred about the free spin g-value, about 24 gauss apart. In this chapter a treatment similar to those of Heller and McConnell is made to try to determine the populations of the rotational levels of methyl radicals trapped

in solid argon at 4.2°K. Let us assume the methyl radicals to be in their planar $^2A_2''$ ground state with the C-H distance 1.08 Å (30). They are thus symmetric tops, of point group D_{3h}, and their rotational energy term values for free rotation are given by:

$$F(J,K) = BJ(J+1) + (A-B)K^2 \qquad (36)$$

where $B = \frac{h}{8\pi^2 c I_B}$; $A = \frac{h}{8\pi^2 c I_A}$; c is the velocity of light; I_A, I_B are moments of inertia about the threefold and twofold symmetry axes respectively; $J = 0, 1, 2 \ldots$; $K = 0, \pm 1, \pm 2 \ldots \pm J$. The lowest levels are given in Table III.

TABLE III

Term Values of the Lowest States of Freely Rotating Methyl Radicals.

J	K	Term value ($cm.^{-1}$)
0	0	0
1	1	14.5
1	0	19.3
2	2	38.6

If freely rotating radicals follow a Boltzmann distribution at 4.2°K, then greater than 99 percent of them will be in the ground rotational state.

Using the Born- Oppenheimer approximation the overall wave function can be written as the product of the electronic, vibrational, rotational and nuclear wave functions (50)(51):

$$\Psi = \Psi_e \Psi_V \Psi_R \Psi_N \qquad (37)$$

Since methyl radicals contain protons, which are fermions of spin $\frac{1}{2}$, the Pauli Principle says that Ψ must be antisymmetric to exchange of two of these protons. Rotation of 180° about one of the twofold axes performs such an exchange, whereas rotation of 120° about the threefold axis is equivalent to exchange of two pairs of protons. Ψ is thus antisymmetric and symmetric respectively to these two operations and is therefore of species A_2 of the rotational subgroup D_3 (51).

The radicals trapped at $4.2^{\circ}K$ may be assumed to be in their ground electronic and vibrational states (symmetry species A_2'' and A_1' respectively). If one now considers the nuclei one finds eight possible different configurations of the three spins, which can be combined into eight orthonormal eigenstates as follows:

$$
\begin{aligned}
\Psi_{N1} &= \alpha\alpha\alpha \\
\Psi_{N2} &= 1/\sqrt{3}\,(\alpha\alpha\beta + \alpha\beta\alpha + \beta\alpha\alpha) \\
\Psi_{N3} &= 1/\sqrt{3}\,(\alpha\beta\beta + \beta\alpha\beta + \beta\beta\alpha) \\
\Psi_{N4} &= \beta\beta\beta \\
\Psi_{N5} &= 1/\sqrt{6}\,(2\alpha\alpha\beta - \alpha\beta\alpha - \beta\alpha\alpha) \\
\Psi_{N6} &= 1/\sqrt{2}\,(\alpha\beta\alpha - \beta\alpha\alpha) \\
\Psi_{N7} &= 1/\sqrt{6}\,(-2\beta\beta\alpha + \beta\alpha\beta + \alpha\beta\beta) \\
\Psi_{N8} &= 1/\sqrt{2}\,(\beta\alpha\beta - \alpha\beta\beta)
\end{aligned}
\qquad (38)
$$

The first four are totally symmetric (species A_1), and correspond to nuclear spins of $^3/_2$, $^1/_2$, $-^1/_2$, $-^3/_2$ respectively. The latter four make up two doubly degenerate states (species E), and correspond to nuclear spins of $^1/_2$, $^1/_2$, $-^1/_2$, $-^1/_2$ respectively. In order for the overall state to be of species A_2, Ψ_R must be of species A_1 when Ψ_N is A_1 (since $A_2 \times A_1 = A_2$), or it must be of species E when Ψ_N is E (since $E \times E = A_1 + A_2 + E$). Of the two most important low lying rotational states being considered here, the state $J=0$, $K=0$ has symmetry A_1, whereas the $J=1$, $K=\pm 1$ level has symmetry E. The $J=1$, $K=0$ state, being of rotational species A_2, is completely absent.

Since there are four A_1 nuclear spin functions, and two E spin functions the A_1 rotational levels have statistical weight 4, whereas the E rotational levels have weight 2.

The intensity of a hyperfine line is proportional to the population of the nuclear level in question. Thus, if the methyl radicals are in the ground rotational state the four hyperfine lines will be in an intensity ratio 1:1:1:1, corresponding to nuclear spins $^3/_2$, $^1/_2$, $-^1/_2$, $-^3/_2$ respectively. However, if the $J=1, K=\pm 1$ rotational state is also populated the intensities of the $^1/_2$ and $-^1/_2$ lines increase and in the limit of both rotational levels being equally populated the intensity ratio reaches 1:3:3:1. This is shown schematically in Figure 10.

4-2 Experimental Methods

Two sources of methyl radicals were employed in the experiments. B and A Reagent Grade methyl iodide was kindly supplied by Dr. G. G. S. Dutton, and although small quantities

of impurities were found by gas chromatography it was used without further purification because of the well known nature of the ESR spectrum of the methyl radical. Dimethyl mercury, the other source, was used without further purification because of its high toxicity. Exhausts from all pumps used in the experiments involving dimethyl mercury were directed either into a fume cupboard or outside. Matheson Research Grade argon was the matrix, and gas mixtures (M/R = 100) were prepared, mixed and deposited in the usual way. The A-H6 lamp was found to be the most effective in preparing the radicals. The spectra were obtained by scanning very slowly over the peaks, with the idea of doing a graphical integration, since the intensity of a transition is proportional to the area under the absorption peak. Microwave power of 5-10 mw. was used, although it was discovered after the experiments were complete that there was a possibility of slight saturation.

4-3 Results and Discussion

The derivative tracings of two of the ESR absorption lines used in the measurements are shown in Figure 11; they are the two highest field peaks of the spectrum. Although a graphical integration was attempted the value obtained for the peak intensity ratio was highly inaccurate because of the large amount of guesswork involved in finding the exact position that a certain slope should be placed. Furthermore, the large tail on either side of the more intense line, which was partly responsible for the large discrepancy, did not fit into the Lorentzian shape of the sharper part of the line and may have been due to a superimposed broad absorption.

To Follow Page 38

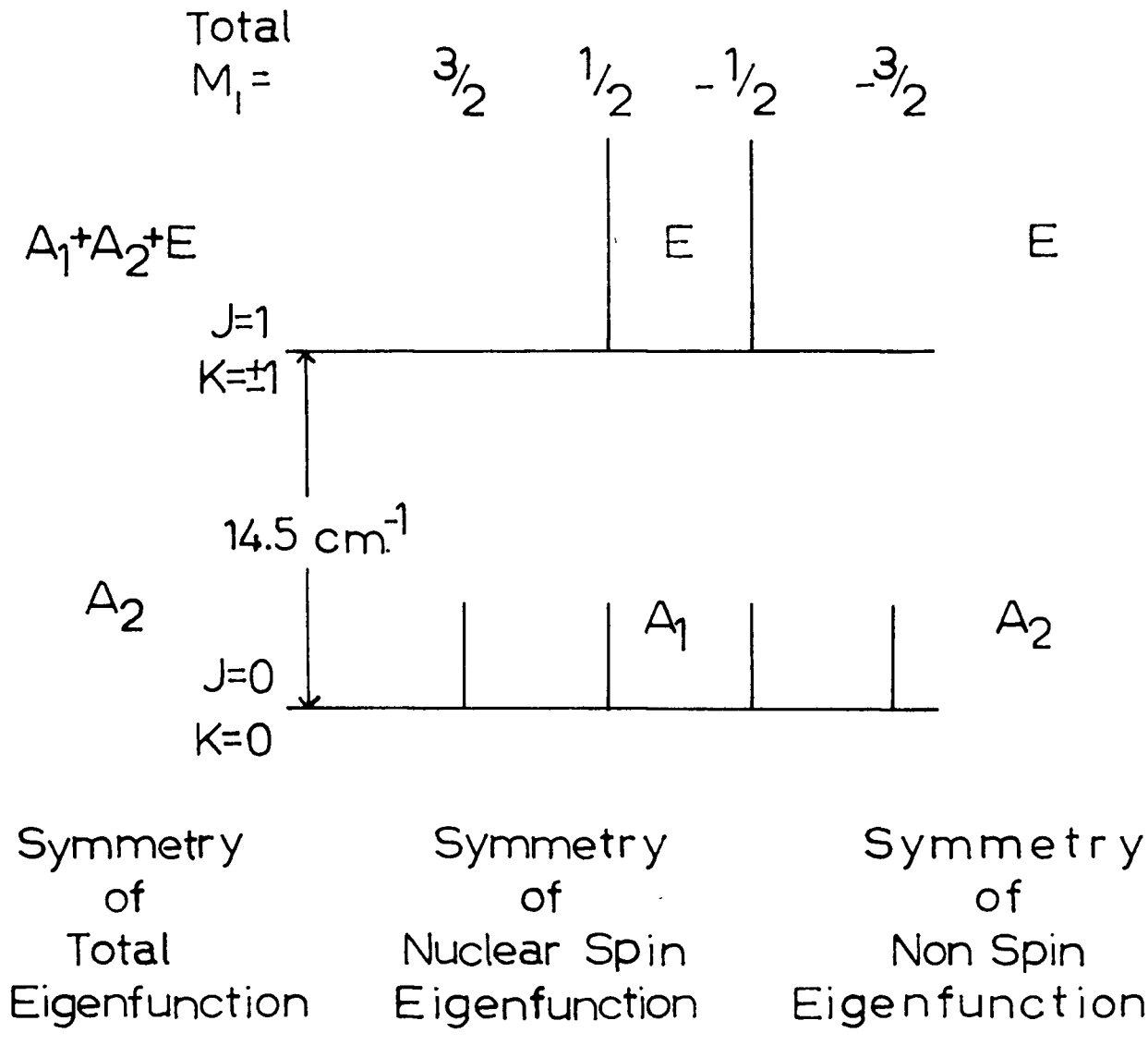

Figure 10. Intensities of the Hyperfine Lines of the ESR Spectrum of the Methyl Radical in its Lowest Rotational Energy States.

To Follow Page 38

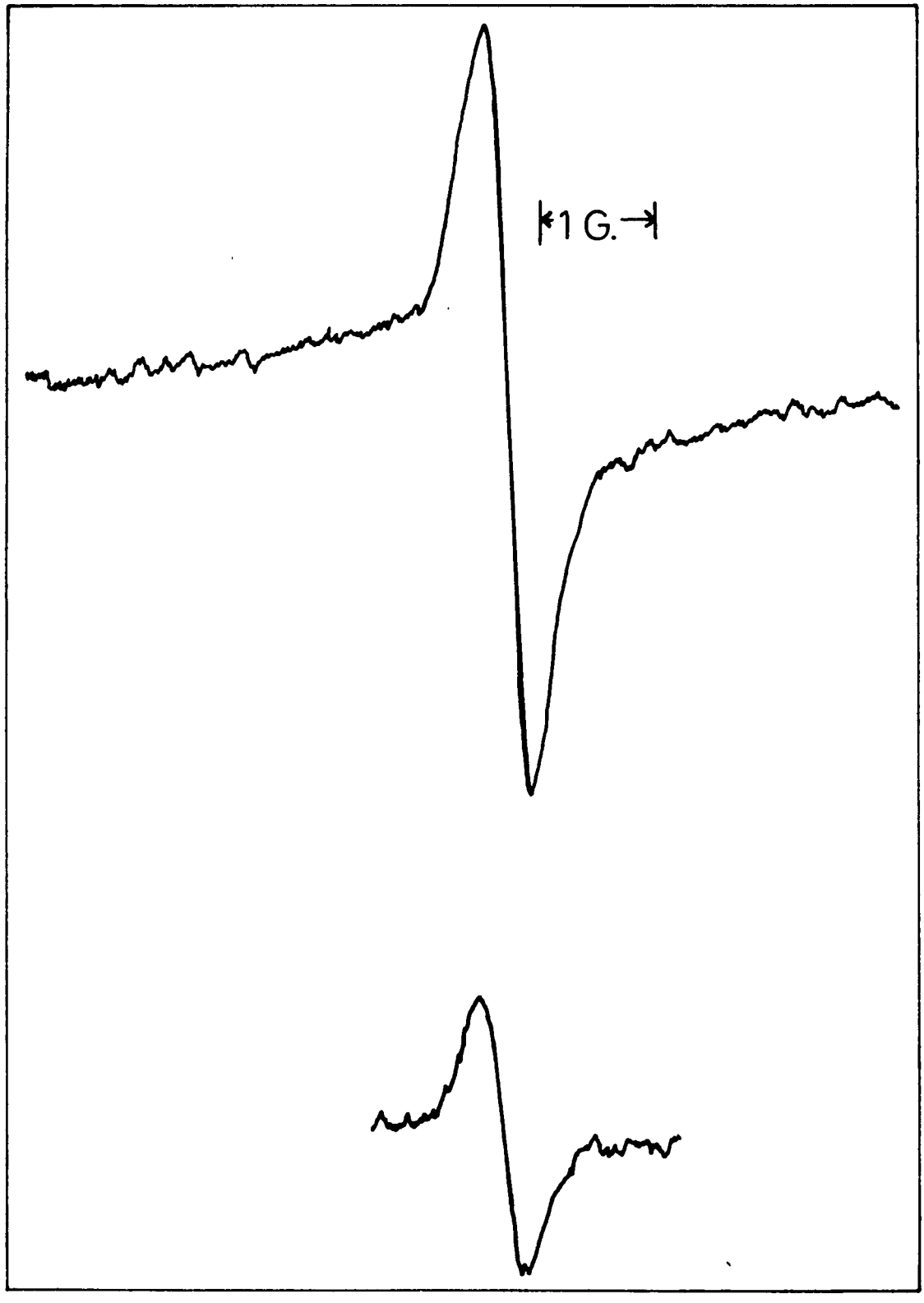

Figure 11. The Two High Field Lines of the ESR Spectrum of the Methyl Radical.

As a result the following procedure was used to determine the absorption intensities. Since both peaks had essentially a Lorentzian line shape, and since both had the same width between the points of maximum and minimum slope, the area under an absorption peak was proportional to its amplitude in the derivative tracing. Thus these heights were measured and found to be in the ratio 2.8:1 for the larger peak to the smaller peak. This ratio may well have been a bit high in favour of the larger peak because of the possibility of a contribution from the superimposed broad absorption. Nevertheless it is quite apparent that the intensity ratio of 1:1, expected if only the ground rotational state of the radicals were populated, was not found, and that many of the radicals were excited above the ground state.

One of the possible reasons why the intensity ratio was not 1:1 is that there was not thermal equilibrium and that the upper rotational level was populated. This was not an impossibility, for if one were to condense a room temperature equilibrium mixture of methyl radicals at $4.2^{\circ}K$ there would be originally a distribution ratio of 1:1 between the two lowest rotational levels (although thermal equilibrium would eventually be achieved). The reason is that combinations between levels of different species (apart from nuclear spin) are forbidden. Now the radicals studied here were prepared at $4.2^{\circ}K$, and although they could all have been produced in the ground state the upper state might easily have been populated as well. In their studies of NH_2 radicals trapped from the gas phase at $4.2^{\circ}K$ Robinson and McCarty (46) found, however, that the room temperature distribution

was not preserved, a fact which they suggested was due to a breakdown of the symmetry selection rule caused by interaction of the nuclear spins with the spin of the unpaired electron. If such a possible situation were achieved in the present experiments, then thermal equilibrium could probably easily have been established.

A very likely cause of the upper rotational level being populated could have been the presence of a potential barrier to free rotation. Effects of such barriers have been considered by Koehler and Dennison (52) for the case of internal rotation of a methyl group in methanol, and by Meyer et al. (38) for the rotation of O_2 in a quinol clathrate. In these cases the two lowest levels came closer together as the potential barrier was increased, and eventually coalesced into part of a vibrational mode. Thus, when the potential barrier was high the upper rotational level could be populated with thermal equilibrium. Now the van der Waals radius of the methyl radical along a CH bond is 2.28 Å, whereas the radius of a substitutional hole in an argon lattice is 1.87Å. Although the van der Waals radius does not necessarily give the effective radius of the radicals, and although the trapping sites of the polycrystalline matrix need not be the substitutional holes, yet nevertheless these figures indicate that if some sort of rotation were occurring, then it was probably greatly hindered. To test this hypothesis it will probably be necessary to reduce the sample temperature considerably, and this will require an apparatus for pumping on the liquid helium to reach temperatures well below the normal boiling point of 4.2°K.

CHAPTER FIVE

THE NF_2 RADICAL

5-1 Introduction

It is now well known that tetrafluorohydrazine, N_2F_4, dissociates into NF_2 radicals at room temperature (53) according to the following equation:

$$N_2F_4 \rightleftharpoons 2NF_2 \quad - \quad 20 \text{ kcal.}$$

Like other polyatomic radicals, NF_2 is expected to exhibit ESR absorption, and such has been observed by Piette *et al.* (54) for NF_2 in the gas phase. The signal observed by them was a single line, of width 104 gauss, centred at g = 2.010, and although hf interactions and coupling of the electron spin with the rotational angular momentum of the radical would be expected in such circumstances, the lack of splitting was explained as being due to a smearing out of the signal by collisional effects.

The N_2F_4 - NF_2 equilibrium has a close analogy in the well known dissociation of N_2O_4 to NO_2. Farmer *et al.* have found that although similar collisional broadening of an NO_2 signal is present at pressures above 5 mm. Hg, NO_2 may nevertheless be trapped in inert matrices and show hyperfine interactions due to the nitrogen nuclear spin (55). A similar study of NF_2 was therefore thought to be feasible. In this case one would expect hyperfine interactions with both the nitrogen ($I_N = 1$) and fluorine ($I_F = \frac{1}{2}$) nuclei, as opposed to only the nitrogen in NO_2, with consequent complication of the spectrum. The study is made more interesting by the lack of data in the literature on fluorine hyperfine interactions, and

it was hoped that a comparison of the hf splittings in NH_2 (3) and NF_2 could be made.

An attempt to detect hf and rotational splittings in the gas phase was also made and is reported in section 5 of this chapter.

5-2 Experimental Method for Trapping the NF_2 Radical

Tetrafluorohydrazine, 99.1% pure, was obtained from Air Products and Chemicals Inc., Allentown, Pa., and, as reported impurities should not interfere in the experiments it was used without further purification. The compound is toxic and under certain conditions may be explosive (56) (57). It was therefore handled in a similar manner to diazomethane, namely using a fume cupboard, with the operator wearing protective clothing. Precautions were taken to keep tetrafluorohydrazine away from organic materials, especially hydrocarbon pump oil, and Kel - F # 90 halocarbon grease was used on the stopcocks. (For the small quantities of tetrafluorohydrazine used Apiezon grease was found satisfactory in the vacuum system where the final gas mixtures for ESR study were prepared.) The matrices used were Matheson Research Grade argon and krypton, as well as Fisher Spectroanalysed carbon tetrachloride. Experiments were carried out at mole ratios (M/R) of 300 and 1200 in both argon and krypton, and 1200 in carbon tetrachloride. Trapping was achieved by depositing the room temperature equilibrium mixture of N_2F_4, NF_2 and matrix gas on the sapphire rod which had been cooled to liquid helium temperature. Such a procedure prevented combination of NF_2 radicals which would otherwise have occurred on cooling. Deposition was continued

until a very high signal-to-noise ratio was obtained.

Spectra were obtained at $4.2^{\circ}K$ and throughout warmup, until the ESR signal disappeared. No appreciable saturation was observed at a microwave power level of one milliwatt and this was used in all the experiments.

Results of an experiment in which NO_2 was trapped at a mole ratio (M/R) of approximately 300 are also described here. The matrix was Matheson Research Grade krypton, and the sample was the room temperature equilibrium mixture of Matheson NO_2 - N_2O_4. The microwave power was one milliwatt.

5-3 Results

(a) Spectra at $4.2^{\circ}K$.

The ESR spectra found for the NF_2 radical trapped in various matrices at $4.2^{\circ}K$ are shown in Figures 12,13,14 and 16. In general all the spectra showed three major lines, with the centre one of greater amplitude but lower peak-to-peak width than the other two. The low field peak had greater amplitude than that at high field, but the two were of comparable width. Numerical data concerning line widths and separations, as well as the g - factor at the point of zero slope of the centre peak,are given in Table IV.

In argon (Figures 12 and 13) some fairly resolvable structure was evident. On the centre line a bump was found at both concentrations approximately five gauss to high field of the point of zero slope, and at M/R = 1200 there was also structure on the low field side of the line three gauss from the same point. (A close look at the spectrum found at M/R = 300 reveals vestiges of this structure). The other two lines were very much smoother,

TABLE IV

Numerical Data from the ESR Spectra of NF_2 Radicals Trapped in Various Matrices at $4.2^{0}K$. This table gives the separations, as well as the line widths between points of maximum and minimum slope, of the three centre lines of the spectra. The g-factor given is that of the point of zero slope of the centre peak.

Matrix	Mole Ratio (M/R)	Low Field Line Width (gauss)	Separation (gauss)	Centre Line Width (gauss)	Separation (gauss)	High Field Line Width (gauss)	g-Factor
Ar	300	5.9 ± 1.0	19.0 ± 1.0	3.3 ± 1.0	17.4 ± 1.0	5.7 ± 1.0	$2.0048\pm.0004$
Ar	1200(A)*	3.3 ± 0.5	16.7 ± 0.5	1.4 ± 0.5	16.3 ± 0.5	2.8 ± 0.5	$2.0050\pm.0004$
Ar	1200(B)*	3.3 ± 0.5	17.4 ± 0.5	1.7 ± 0.5	16.9 ± 0.5	4.9 ± 0.5	$2.0054\pm.0004$
Kr	300	8.5 ± 0.5	19.4 ± 0.5	3.3 ± 1.0	16.3 ± 0.5	9.0 ± 0.5	$2.0047\pm.0004$
CCl_4	1200	-#	11.7 ± 0.5	7.7 ± 0.5	17.2 ± 0.5	-#	$2.0049\pm.0004$

* Two experiments were carried out in argon at M/R = 1200.

These line widths are unspecified because of the nebulous nature of the peaks (see Fig. 16).

To Follow Page 44

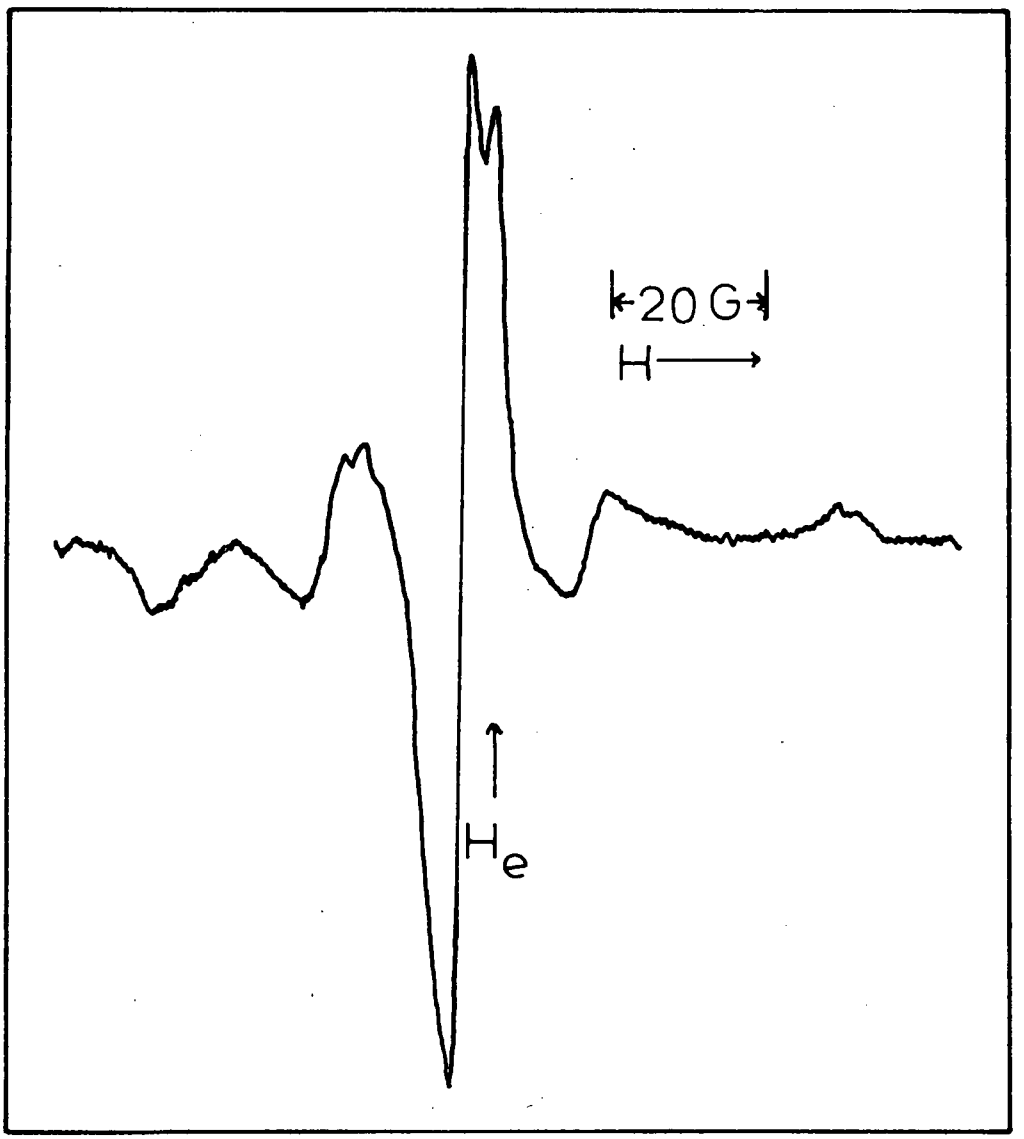

Figure 12. ESR Spectrum of NF_2 in Argon (M/R = 300) at 4.2°K.

G denotes gauss. H_e is the magnetic field where g=2.0023.

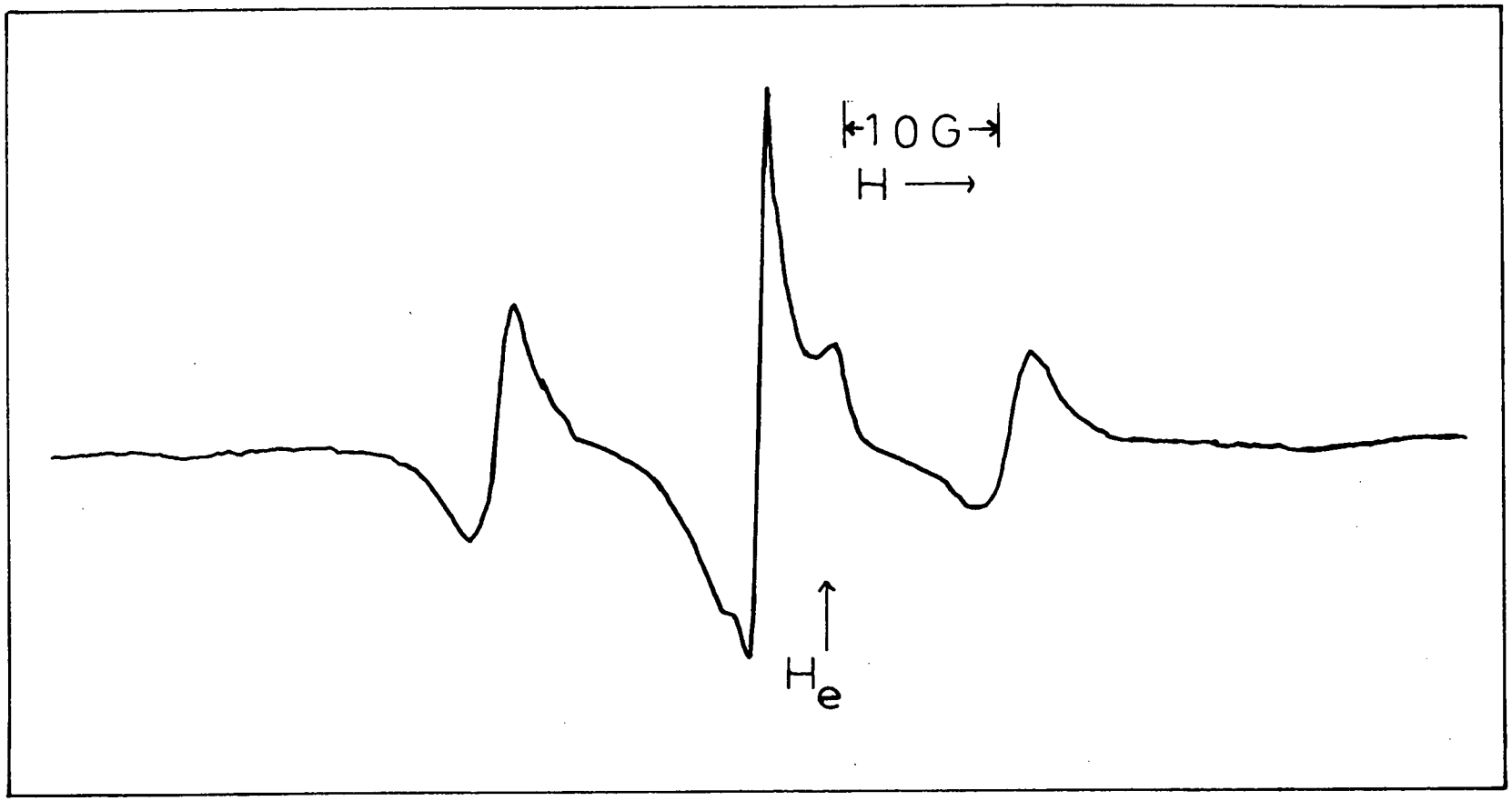

Figure 13. ESR Spectrum of NF_2 in Argon (M/R=1200) at 4.2°K.
G denotes gauss. H_e is the magnetic field where g=2.0023.

To Follow Page 44

To Follow Page 44

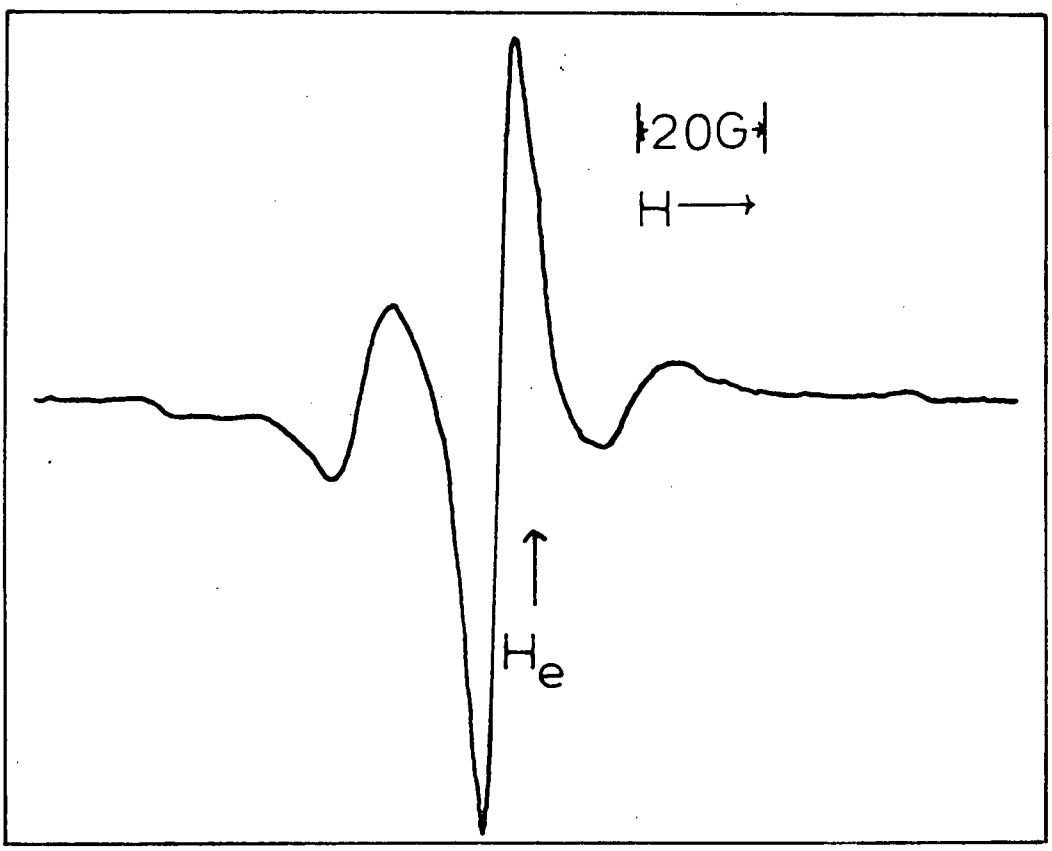

Figure 14. ESR Spectrum of NF_2 in Krypton (M/R=300) at 4.2°K. G denotes gauss. H_e is the magnetic field where g= 2.0023.

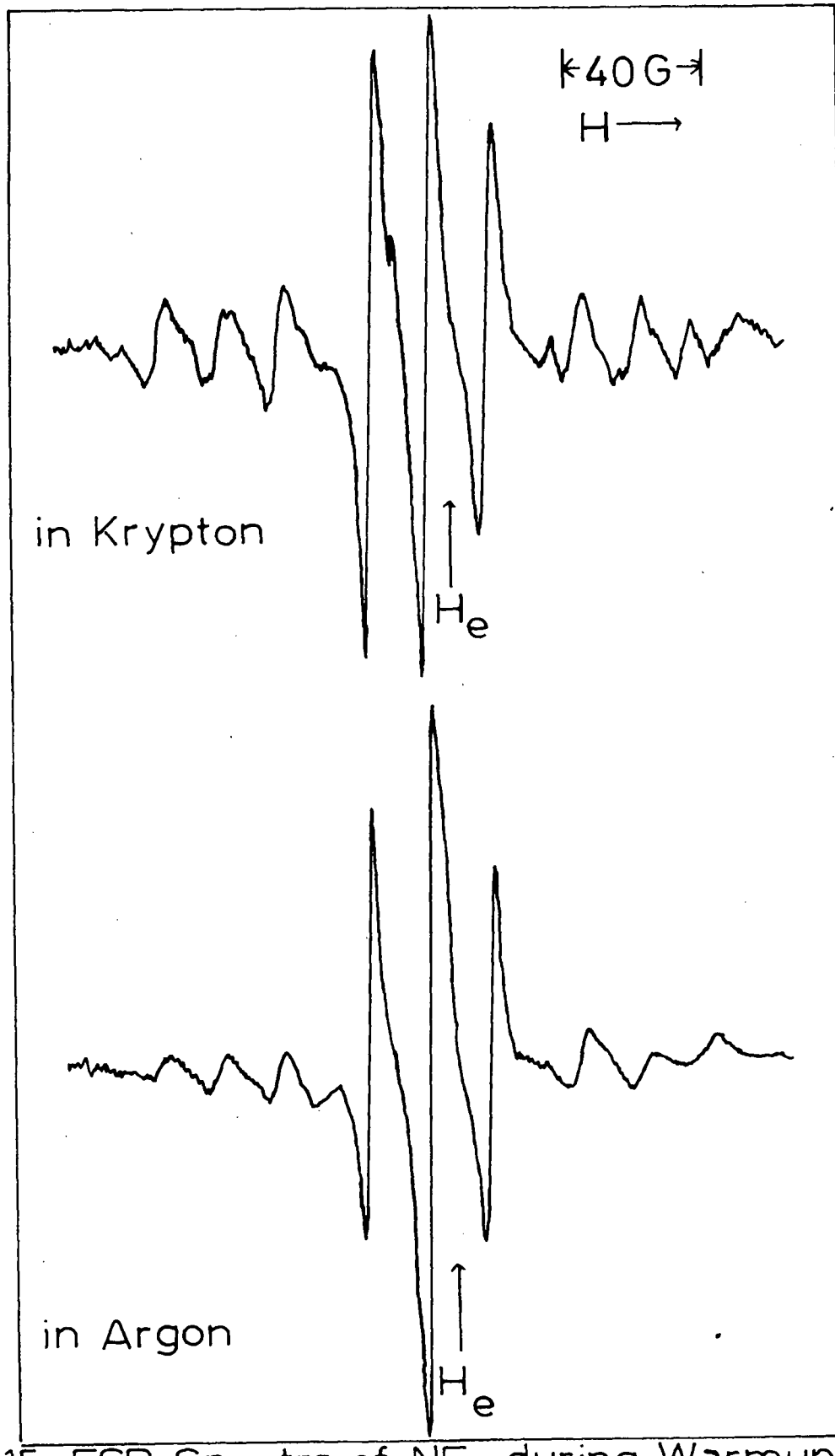

Fig. 15. ESR Spectra of NF_2 during Warmup.

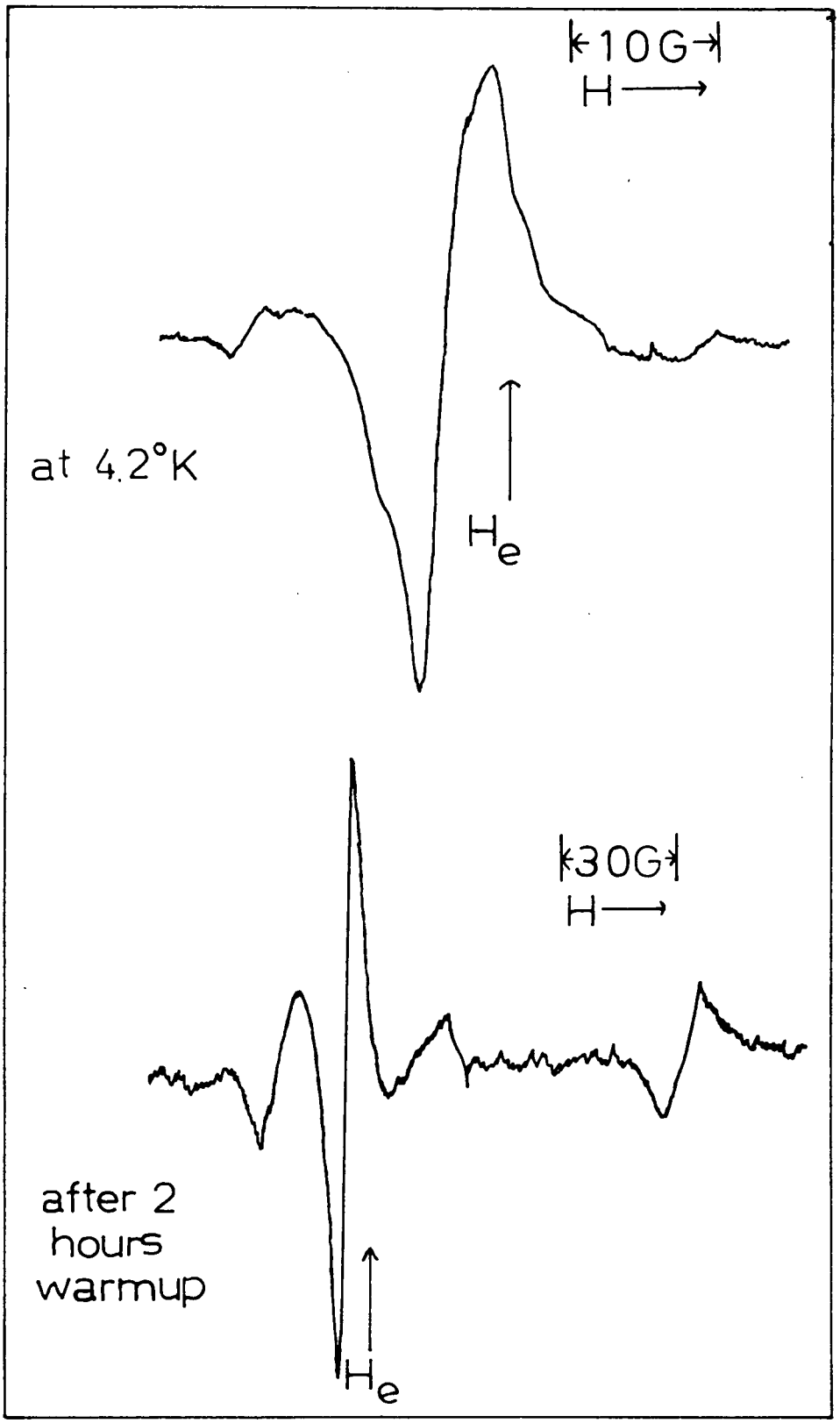

Figure 16. ESR Spectra of NF_2 in CCl_4 (M/R=1200). G denotes gauss. H_e is the magnetic field where g=2.0023.

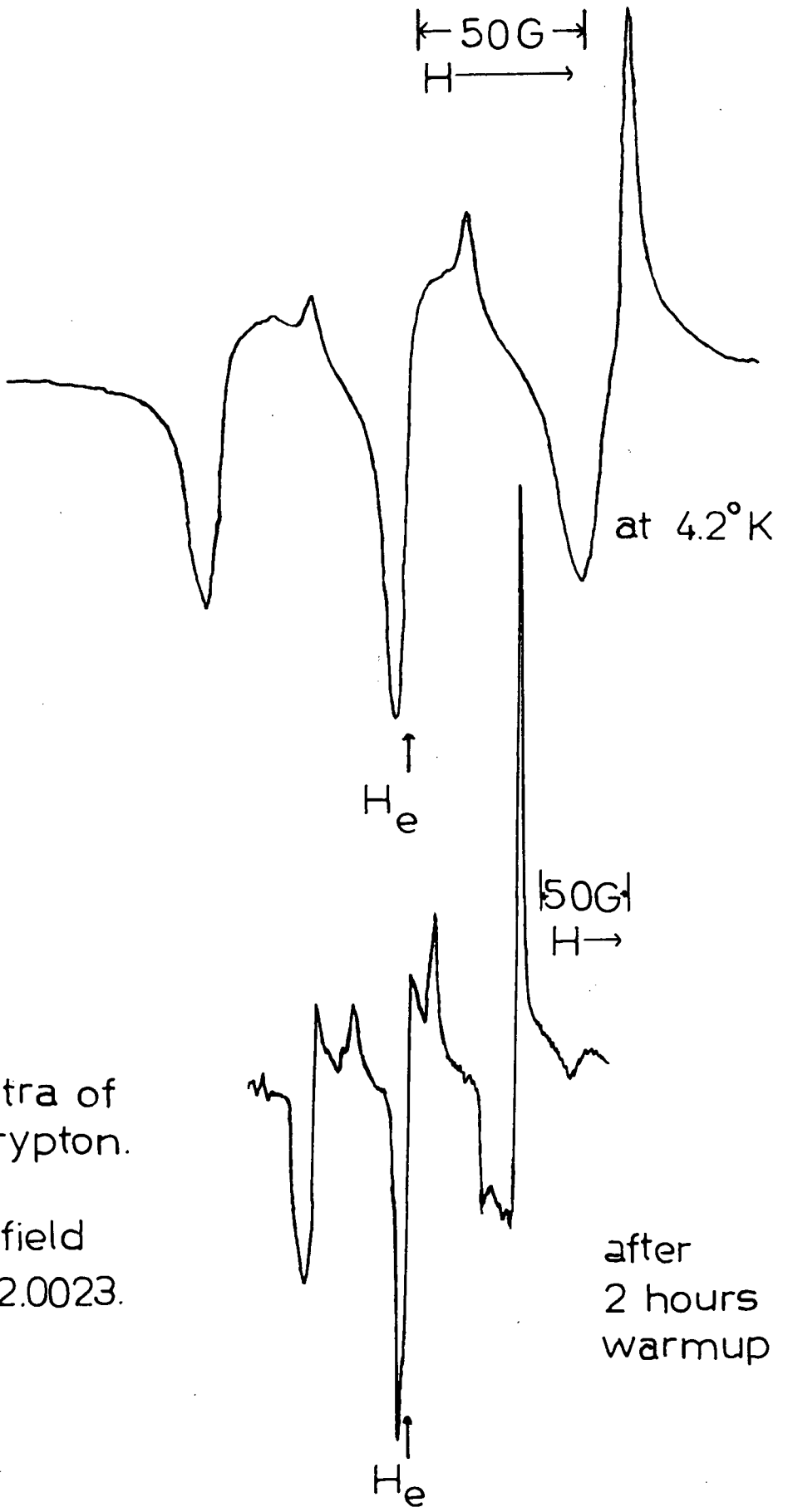

Figure 17.

ESR Spectra of NO_2 in Krypton.
G = gauss.
H_e is the field where g=2.0023.

although there was some structure on the low field peak at M/R = 300. It is interesting to note from the above table that at M/R = 1200 the peak-to-peak widths were in general about half those at M/R = 300. However data changed considerably from run to run on the same sample (see the two high field peak widths in argon at M/R = 1200), and so probably little conclusion can be drawn from this observation. The divergence in the two peak widths just citedwas probably due to slight differences in deposition conditions, although they were supposedly the same.

In krypton (Figure 14) much of the structure was absent. On the centre line the bump to high field was reduced to a shoulder, while the ones on the low field side of the centre peak and on the low field peak were missing. It is possible in this case that averaging of the anisotropic parts of the hf interactions and g - factor may have been appearing because of the probable larger size of the krypton trapping sites than the argon sites.

At M/R = 300 in the inert gas matrices two further absorptions could be seen, one on either side of the main triplet. There were two very noticeable features of these lines : (a) The one at high field was further from the centre than the one at low field. (b) Neither peak crossed the baseline, suggesting that they were due to a broadening of the main absorption rather than individual transitions.

The spectrum obtained when NF_2 was trapped at liquid helium temperature in carbon tetrachloride was very much distorted in comparison to those found in the inert gases (see

Figure 16). The two outer peaks of the triplet, compared to the centre one, were very weak indeed, and the centre peak was very distorted, being of a peculiar shape and very much wider than that found in argon and krypton. Also, the centre-to-centre separation of the low field and centre lines was 12 gauss, as opposed to approximately 18 in the inert gases. However the g - factor at the point where the centre peak crossed the baseline was 2.0049 ± .0004, the same as in the inert gases.

(b) Warmup Spectra

Essentially the same changes were observed during warmup in both the argon and krypton matrices. The peak-to-peak widths of the two outer lines decreased, their amplitutes increased and the bumps on the centre peak faded. Apparently any anisotropies of the g - factor and the hf interactions were being averaged out, and it is probable that with less rigidity in the lattice the radicals were beginning to rotate. It became apparent that in the limit of isotropic rotation the three lines, now 17±1 gauss apart and centred about g = 2.0053 ± .0006, would be of equal intensity and they were therefore assigned to hf interaction with a nucleus of spin one , namely nitrogen - 14.

Warmup spectra in both argon and krypton are shown in Figure 14. It will be noticed that besides the centre triplet there are two further triplets, one on each side of the centre one, neither of which was observed at 4.2°K. The individual lines of each triplet are 17 ± 2 gauss apart and the centre line

of each triplet is 60 ± 2 gauss from the centre line of the spectrum. An assignment of the interaction of 60 ± 2 gauss to the isotropic hf interaction constant for the fluorine atom was suggested. Now, if this were the correct assignment the amplitude ratio of the outer triplets to the main one would be expected to be 1:2:1. That found was somewhat greater, but the transient nature of the spectrum, the fact that the lines of the outer triplets were somewhat wider than those of the main triplet, and the constancy of the splittings all tend to overrule this objection, and the assignment is probably valid.

In carbon tetrachloride the signal intensity decreased steadily during warmup, but there was no sign of the structure found in the inert gases. Figure 16 shows the signal obtained about two hours after the start of warmup. The intensities of the two outer peaks relative to the centre one were very much greater; also there was a peak, not observed at 4.2°K, about sixty gauss to high field of the triplet. The origin of this peak is unknown, but it was probably caused by an impurity. It was still present many hours after warmup had started, when the cavity was at 77°K, and after the triplet had disappeared.

(c) NO_2 Trapped in Krypton

After probable averaging of anisotropies in the hf interaction and the g-factor had been observed for the NF_2 radical during warmup, an experiment was carried out to see if the same could be observed for NO_2 in krypton. The spectrum obtained at 4.2°K (Figure 17) was very similar to that found in other matrices (11)(55). Throughout warmup, however, the structure,

unlike that of the NF_2 radical, did not disappear, and it seems that the anisotropies remained.

5-4 Discussion

Let us consider the signals obtained at $4.2^{\circ}K$ in the light of the warmup spectra found in the inert gases. If it is assumed that all hf and g - factor anisotropies were averaged out in the warmup spectra equation (18) is applicable in discussing transitions, and should be written for the case of NF_2 as follows:

$$h\nu = g\beta H_0 + \sum_F A_F (M_I)_F + A_N (M_I)_N \qquad (39)$$

where $(M_I)_F$ and $(M_I)_N$ are components of the nuclear spins of fluorine and nitrogen nuclei; A_F and A_N are the isotropic hf splitting constants of fluorine and nitrogen respectively. Now in NF_2 there are two fluorine - 19 atoms of nuclear spin $\frac{1}{2}$ and one nitrogen - 14 atom of nuclear spin 1. Thus both $\sum_F (M_I)_F$ and $(M_I)_N$ can have values 1,0, - 1 and equation (39) predicts nine transitions. It indicates also that the three nitrogen peaks should be superimposed on each of the three due to fluorine or *vice versa*. The high intensity of the centre triplet compared with the other two indicates that the former is the case for the NF_2 radical. Now if the anisotropic part of the hf splitting were to have an influence the outer triplets should show effects of both the fluorine and nitrogen anisotropy, whereas the main one should show only those due to nitrogen anisotropy. Furthermore for the centre line of the main triplet both $\sum_F (M_I)_F$ and $(M_I)_N$ should be zero, so that the hf interaction should have no effect on it whatsoever.

These inferences appear to be justified in the spectra obtained at 4.2°K. The two outer peaks of the triplet have been observed to be of greater width and smaller amplitude than the centre line, consistent with the suggestion that the outer peaks can be influenced by anisotropy of the nitrogen hf interaction whereas the centre one cannot. Furthermore the narrowness of the centre line tends to discount other forms of broadening. The fact that on warmup the line widths of the outer peaks decreased whereas their amplitudes increased adds further impetus to the suggestion. If one carries the inference further it appears that the anisotropic part of the fluorine hf interaction is very large, so large in fact that it can broaden the isotropic part beyond detectability at 4.2°K. On warmup, however, it is averaged out. It may be pointed out in passing that Gordy *et al.* (58)(59)obtained structure in a signal at room temperature from X - irradiated teflon which they assigned to fluorine hf interactions; this structure was broadened considerably at 90°K, a phenomenon rather similar that observed here for NF_2.

The structure of the centre peak found for NF_2 trapped in argon may be related to anisotropy in the g - factor tensor. Kneubuhl (15) has shown how the line shape of an ESR signal of randomly oriented radicals in which there is no hf splitting can be related to the principal values of the g - factor tensor. Adrian *et al.* have used his calculations to determine these values for NO_2 (11) and DCO (10). Now the line shape found for NF_2 was somewhat different from those shown by Kneubuhl and by

Adrian, but the structure may be similarly related to the g - factor.

Some interesting comparisons can be made between the spectra of NO_2 and NF_2. The ESR spectrum of trapped NO_2 has very definite structure which can be related to the g - factor and hf anisotropies (11). In argon the spectrum shows NO_2 to be axially symmetric, although it need not necessarily be so, and Adrian postulated slight hindered rotation of the NO_2 to account for this. An attempt to do a similar treatment for NF_2 ended in failure because of the great width and smoothness of the outer peaks of the triplet. Indeed, the smoothness of the lines suggests slow, rather isotropic rotation of the radicals, and the ease with which the peaks sharpened on warmup tends to corroborate this idea.

It is also interesting that on warmup the hf anisotropy failed to be averaged out for NO_2 but was apparently removed for NF_2. Now removal of the hf anisotropy requires a tumbling frequency $\omega \gg B/\hbar$, B being the anisotropic hf splitting constant. For nitrogen in NO_2 $B/\hbar$ is 21 ± 3 mc./sec., so that during warm-up NO_2 never underwent tumbling motion of frequency greater than this. On the other hand for fluorine in NF_2 $B/\hbar$ must be much greater than this, in order to broaden the isotropic part beyond detectability, yet during warmup it was averaged out quickly in both argon and krypton.

A clue to the causes of these interesting phenomena may be in the shapes and sizes of the two radicals. NO_2 is somewhat more elongated and more bulky than NF_2, for its bond angle is

$134^{\circ}\ 15'$ with N - O length of 1.197 Å, whereas the bond angle in NF_2 is 104.2° if the N - F distance is 1.37 Å (60). Using the van der Waals radii for N, F and O of 1.5, 1.35 and 1.40 Å respectively (61) one obtains approximate isotropic van der Waals radii of 2.7 and 2.4 Å for NO_2 and NF_2 respectively. These figures may have some bearing on the apparent ease of NF_2 to undergo isotropic motion in comparison with the difficulty of NO_2.

The two outer peaks in the M/R = 300 spectra at $4.2^{\circ}K$ are noteworthy in that they apparently did not appear at higher matrix ratios and that they did not cross the baseline. It is very possible that they were due to broadening of the main triplet and may have been a sign of peaks found during warmup.

A rather curious similarity is found in comparing the centre triplet of NF_2 with the spectrum of trapped CN radicals (12). Both showed a triplet, with the centre line of very much greater amplitude than the other two, and with the outer lines broad but smooth. Furthermore, in both the outer lines narrowed and increased in amplitude during warmup. The line separations were different, of course, but the similarity of the spectra is remarkable.

The spectra obtained in carbon tetrachloride were very strange. This was one of the first times that this matrix had been used at $4.2^{\circ}K$. Because of its high melting point a lengthy study of the warmup spectra found for the inert gases was hoped for, but this was not to be. The small intensity of the outer peaks of the main triplet, along with the absence of the outer triplets during warmup suggests less rotational freedom

for the radicals here than in other matrices. The freezing point of carbon tetrachloride is much higher than those of argon and krypton, and it is consequently more rigid than these at $4.2^{\circ}K$. This was probably the main cause of the observed broadening, although it should be mentioned that enough motion of the matrix was found to allow diffusion and hence recombination of the radicals.

Let us now compare the isotropic spectrum of NF_2 with the spectrum of NH_2 (3). For NF_2 the observed splittings of 17 ± 1 gauss and 60 ± 2 gauss for the nitrogen and fluorine hf interactions correspond to isotropic hf onstants of 48 ± 3 and 168 ± 6 mc./sec. respectively. In NH_2 these are 28.9 and 67.0 mc./sec. for nitrogen and hydrogen respectively. Now the isotropic hf splitting constant for nucleus j, after integration over the spatial part of the wave function, is given by

$$A_j = \frac{8\pi}{3} g \beta g_j \beta_I |\psi_j(0)|^2 \qquad (40)$$

where g_j and β_I are the nuclear g-factor of nucleus j and the nuclear magneton respectively, and $\psi_j(0)$ is the value of the unpaired electron wave function at nucleus j. The nuclear g-factors for fluorine-19 and hydrogen are approximately equal, being 5.25 and 5.6 respectively, and with the other factors in A_j being numerical constants any differences in the isotropic hf constants must arise mainly from the $|\psi_j(0)|^2$ term. Now the unpaired electrons in both NH_2 and NF_2 are both expected to be in orbitals having the molecular plane as a nodal plane (20). Since A_j would be zero if the electron were purely in such an

orbital, the true orbital must have some s-character to give a non - zero constant. This is usually explained by admixing the ground state by configuration interaction with an excited state in which the unpaired electron is in an orbital with some s-character.

Isotropic hf interaction due to the hydrogen nuclei in NH_2 results from the unpaired electron being in an orbital with some hydrogen 1s-character. If this orbital were purely the 1s of hydrogen the hf constant would be 1420 mc./sec. It is actually 67 mc./sec. Thus, in the molecular wave function the degree of 1s-character from each hydrogen atom may be considered to be 4.7 percent. On the other hand the fluorine atoms in NF_2 have a 2s orbital available and since excited states with the unpaired electron in the 1s state would be of much higher energy than those with it in the 2s orbital configuration interactions will be assumed to involve excited states with the unpaired electron in the latter. Using the self - consistent field wave functions of Brown (62) for the fluorine atom one finds that $|\Psi_F(0)|^2$ is 68×10^{24} cm.$^{-3}$ for the fluorine 2s state, so that if the electron were purely here the splitting constant would be 42,500 mc./sec. As it is actually 168 mc./sec. the molecular wave function may be said to have fluorine 2s-character to the extent of 0.4 percent from each fluorine atom.

For nitrogen, which also has a 2s orbital available, the configuration interaction is again most likely to involve excited states with the unpaired electron here. From the self - consistent field calculation of Hartree and Hartree (63) the value of $|\Psi_N(0)|^2$ for the 2s orbital of atomic nitrogen may be estimated as 33×10^{24} cm.$^{-3}$ Since the g-factor of nitrogen-14 is 0.40

this gives a splitting constant of 1540 mc./sec. For NH_2 and NF_2 the constants are 28.9 and 48 mc./sec. giving the molecular wave functions 1.9 and 3.1 percent nitrogen 2s-character respectively.

5-5 A Gas Phase Study of the NF_2 Radical

Although Piette et al. (54) found a gas phase spectrum of NF_2 the absorption was very broad, and showed no sign of structure, in spite of the fact that the unpaired electron spin should couple with the spins of both the nitrogen and fluorine nuclei and also with the rotational angular momentum of the radical. The lack was due to collisional effects at the pressure used, and it was felt that the structure should be observable at a lower pressure. Previous work of Farmer in this laboratory had shown this to be so for the case of NO_2, and accordingly an attempt was made to find such structure in NF_2.

Air free samples had to be prepared very carefully, as the slightest traces of paramagnetic oxygen molecules can broaden the structure of the ESR spectrum of the NF_2, present in very low concentrations, beyond detectability. The silica sample tubes, and especially the constriction where the tubes were sealed, were heated to 400°C and continuously pumped for at least four and usually eight hours to remove all traces of oxygen. After this operation the sample tube was filled with the N_2F_4 - NF_2 equilibrium mixture to the pressure desired and the tube was then sealed with a blowtorch. During these operations, all done in a fume cupboard, the operator wore a face mask and heavy protective clothing to guard against

possible explosions.

A multipurpose ESR spectrometer with field modulation at 100 kc./sec. was used in these studies. The first sample investigated was prepared in 10 mm. tubing with the N_2F_4 - NF_2 equilibrium mixture at 3 - 10 mm. Hg pressure, and was run at room temperature. There was no sign of the broad signal reported by Piette et al., and since he found his first signal well above room temperature all further studies were carried out at temperatures above ambient. The Varian V - 4547 Variable Temperature Accessory was used to raise the temperature. Nitrogen from a cylinder was passed through a calcium chloride drying tube, heated by a coil and passed through a dewar into the cavity. The temperature was monitored with a copper - constantan thermocouple at the entrance to the cavity. The sample tubes used were 4 mm. silica.

The results of the high temperature experiments at various pressures are shown in Table V. It is apparent that no structure was found at the pressures used and that the signal would be lost in the noise at any pressures lower than 3 mm. Hg. Probably there were simply not enough radicals present in the tube. Now an equilibrium calculation at 300°C indicates that tetrafluorohydrazine is almost completely dissociated at that temperature, so an explanation of the weak signal must be found elsewhere.

It is likely that at the high temperature used the tetrafluorohydrazine was attacking the silica tube, especially if there were any very slight traces of water or possibly

TABLE V

Results of high temperature experiments involving the NF_2 radical in the gas phase.

Pressure at Room Temperature	Result
15 cm. Hg	nil
10 mm. Hg	Weak signal, 34-68 gauss wide superimposed on the general drift, about g = 2.017±.001. Intensity increased from 167° to 207°C. No structure.
3mm. Hg	Same signal, much weaker - nearly lost in noise, even at temperatures up to 300°C. No structure.

hydrogen fluoride present. Water could easily have been there, since the tetrafluorohydrazine was stored in a glass trap *in vacuo* at room temperature prior to use. At the high temperatures in the sample tube the tetrafluorohydrazine was probably disappearing and being replaced by SiF_4. If this were the case then the small signal was probably due to lack of NF_2 radicals in the sample tube.

CHAPTER SIX

THE TRIFLUOROMETHYL RADICAL

6-1 Introduction

Attempts were made to trap the trifluoromethyl radical (CF_3) in an inert matrix at $4.2^{\circ}K$. The method used was to irradiate CF_3I trapped in the solid with the hope that the C-I bond would break in similar fashion to the same bond in methyl iodide. That this bond should break on irradiation was suggested by photolysis (64) and pyrolysis (65) experiments with gaseous CF_3I.

Previous attempts to trap the CF_3 radical have been made. Florin *et al.* (66) carried out ESR studies of gamma irradiated solid CF_4. At $77^{\circ}K$ they found a four line signal very similar to that of the methyl radical, while at $4.2^{\circ}K$ their spectrum was so complicated that it defied interpretation. Mastrangelo (67) trapped the products of a microwave discharge in C_2F_6 at $77^{\circ}K$ and used chemical data to identify one of the deposition products as the CF_3 radical.

6-2 Experimental Method

Dr. W. R. Cullen kindly supplied the CF_3I used in these experiments. The very small quantities of impurities were removed in a Perkin-Elmer Vapor Fractometer, and air was removed by distillation *in vacuo*. Matheson Research Grade argon and krypton, as well as Fisher Spectroanalysed carbon tetrachloride, were the matrices, and the mole ratios (M/R) were 100, 100, and 60 - 75 respectively. Mixing and sample deposition were carried out in the usual way. The H85A3/UV lamp was found

to be the most successful in preparing the radicals. The field region of g = 2 was scanned, and microwave power levels of about 1 - 10 mw. were used.

6-3 Results and Discussion

Only weak signs of a signal were obtained when CF_3I trapped in argon was irradiated. However in krypton and carbon tetrachloride spectra were obtained easily and are shown in Figures 18 and 19. Their most striking features were the great overall width and complexity, and also the presence of lines in which there was apparently a phase reversal (i.e. they appeared as though they were due to emission rather than absorption).

The cause of the reversed peaks is unknown. Possibly they were related in some way to the spin-lattice relaxation time T_1 (the time in which an initial excess of energy given to the spins will fall to $1/e$ of its value), perhaps in a similar fashion to the peaks of atomic hydrogen found by Jen et al. (5). They found the absorption signal to have a component lagging the modulation frequency by 90°, which they felt was due to the modulation frequency being of the order of magnitude of $1/T_1$. How much influence this had in the present case is uncertain at the time of writing. However one further point should be made. When carbon tetrachloride was used as the matrix there was a small piece of diphenylpicrylhydrazyl (D.P.P.H.) on the target which gave a superimposed signal. During warmup the phase of the entire signal, except for the D.P.P.H. line, was reversed indicating that either the motion of the matrix or the temperature had a very profound influence on the spectrum.

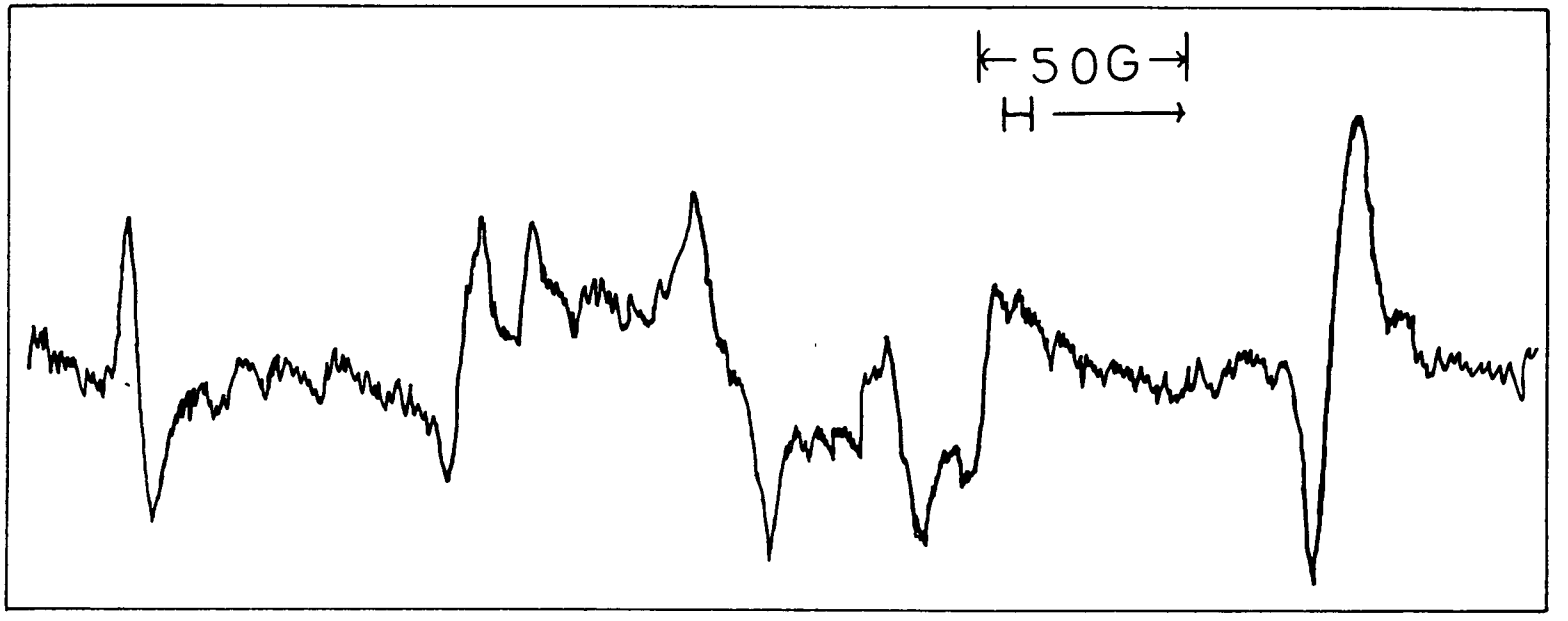

Figure 18. ESR Spectrum Obtained on Irradiation of CF_3I in Krypton (M/R=100) at 4.2°K. G denotes gauss.

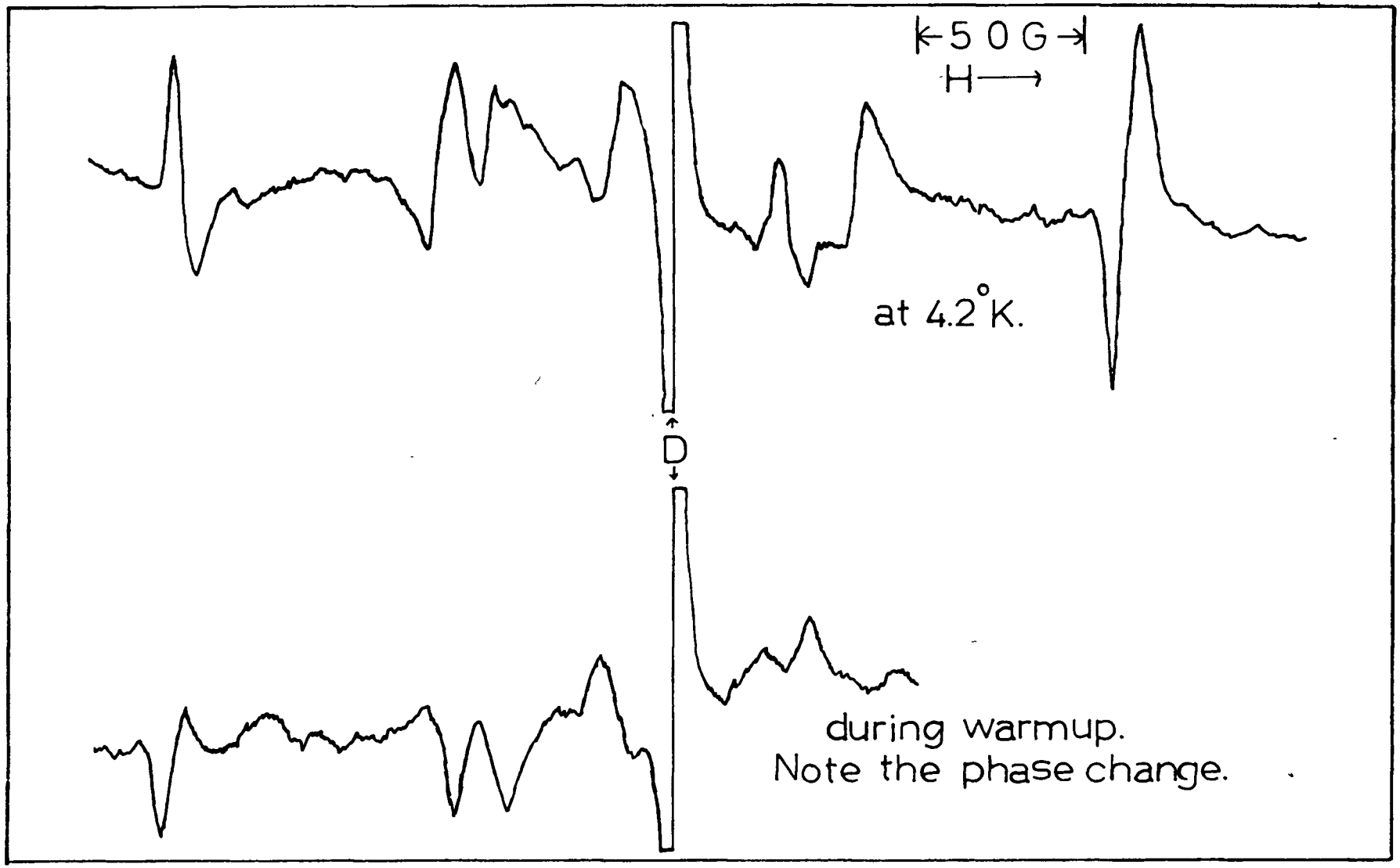

Fig.19. ESR Spectra Obtained on Irradiation of CF_3I in CCl_4 (M/R=60-75). The line marked "D" is due to D.P.P.H. G=gauss.

In later attempts to reproduce the results difficulty was encountered in obtaining a signal.

Complete assignments of the lines must await an explanation of the phase reversal. Inspection of the spectrum revealed little apparent system (expected were four lines of rather the same pattern as that for the methyl radical). It may possibly be that more than one radical was involved, and if they had different relaxation times then one may be able to account for the phase shift. Suffice it to say, however, that the great overall spread of 288 gauss was consistent with the large spreads found for other fluorine compounds (58)(59) (see also chapter 5.)

It may also be mentioned in passing that a sample of 15 percent CF_3I in carbon tetrachloride was irradiated at 77°K with the A-H6 lamp. The sample was held in a piece of 4mm. silica tubing and was cooled in a Varian V-4546 Liquid Nitrogen Accessory. A single ESR line was observed, of peak-to-peak width 23.0 ± 0.5 gauss at $g = 2.009 \pm .001$. The signal disappeared on warmup, and the purple colour of molecular iodine was observed in the solution at room temperature. This result was quite different from that obtained at 4.2°K, and reemphasized the need for further work on the system.

CHAPTER SEVEN

CONCLUSIONS

The scope of the experiments just described seems to be rather limited. The reason for this statement is that the technique appears to be restricted to the study of small free radicals, since in larger ones anisotropic hf broadening is often so great as to make interpretations of the spectra very difficult, if not impossible. Furthermore the large cage effect of the matrix makes quantum yields for photolyses in situ very small. Since the supply of liquid helium is limited in each experiment studies of most radicals have to be made at signal-to-noise ratios rather lower than desirable. This statement does not include two important types of experiments, for which fruitful studies can be made, namely those involving ready made radicals like NF_2 which can be deposited from the gas phase and those involving the photolysis of compounds like diazomethane, in which one of the fragments is a stable molecule.

A possible method of overcoming the quantum yield difficulty may be to use high energy radiation. The lamps used in the experiments were medium and high pressure mercury arcs, with the result that high energy resonance radiation was self - absorbed. Use of a low pressure resonance lamp would probably increase the quantum yield.

Deposition of radicals prepared in the gas phase (with the use of high intensity ultraviolet radiation or a microwave discharge) would also overcome the quantum yield difficulty for here the cage effect would be absent. However, for this type of experiment the apparatus must be completely redesigned.

BIBLIOGRAPHY

1. G. C. Pimentel, Formation and Trapping of Free Radicals, ed. A. M. B ass and H.P. Broida.New York, Academic Press, 1960, chapter 4.

2. C.K. Jen, S.N. Foner, E.L. Cochran and V.A. Bowers, Phys. Rev., 104, 846 (1956).

3. S.N. Foner, E.L. Cochran, V.A. Bowers and C.K. Jen, Phys. Rev. Letters, 1, 91 (1958).

4. S.N. Foner, C.K. Jen, E.L. Cochran and V.A. Bowers, J.Chem. Phys., 28, 351 (1958).

5. C.K. Jen, S.N. Foner, E.L. Cochran and V.A. Bowers, Phys. Rev., 112, 1169 (1959).

6. E.L. Cochran, V.A. Bowers, S.N. Foner and C.K. Jen, Phys. Rev. Letters, 2, 43 (1959).

7. S.N. Foner, E.L. Cochran, V.A. Bowers and C.K. Jen, J. Chem. Phys., 32, 963 (1960).

8. F.J. Adrian, J. Chem. Phys., 32, 972 (1960).

9. E. L. Cochran, F.J. Adrian, and V.A. Bowers, J.Chem. Phys., 34, 1161 (1961).

10. E. L. Cochran, F.J. Adrian and V.A. Bowers, J. Chem. Phys., 36, 1661 (1962).

11. F. J. Adrian, J. Chem. Phys., 36, 1692 (1962).

12. E. L. Cochran, F.J. Adrian and V.A. Bowers, J. Chem. Phys., 36, 1938 (1962).

13. S.M. Blinder, J. Chem. Phys., 33, 748 (1960).

14. S. I. Weissman, J. Chem. Phys., 22, 1378 (1954).

15. F. K. Kneubuhl, J. Chem. Phys., 33, 1074 (1960).

16. W. H. Duerig and I.L. Mador, Rev. Sci. Instr., 23, 421 (1952).

17. J. M. Foster and S.F. Boys, Revs. Mod. Phys., 32, 305 (1960).

18. J. E. Lennard-Jones, Trans. Faraday Soc., 30, 70 (1934).

19. R. S. Mulliken, Phys. Rev., 43, 279 (1933).

20. A. D. Walsh, J. Chem. Soc., 2253 (1953).

21. P.C.H. Jordan and H.C. Longuet-Higgins, Mol. Phys., 5, 121 (1962).

22. J. B. Pedley, Trans. Faraday Soc., 58, 23 (1962).

23. P. S. Skell and R. C. Woodworth, J. Am. Chem. Soc., 78, 4496 (1956).

24. F.A.L. Anet, R.F.W. Bader, and A.M. van der Auwera, J. Am. Chem. Soc., 82,3217 (1960).

25. H . M. Frey, J.Am.Chem. Soc., 82, 5947 (1960).

26. D. E. Milligan and G. C. Pimentel, J. Chem. Phys., 29, 1405 (1958).

27. T. D. Goldfarb and G. C. Pimentel, J. Chem. Phys., 33, 105 (1960).

28. T. D. Goldfarb and G. C. Pimentel, J. Am. Chem. Soc., 82, 1865 (1960).

29. G. W. Robinson and M. McCarty, J. Am. Chem. Soc., 82, 1859 (1960).

30. G. Herzberg, Proc. Roy. Soc. (London), A262, 291 (1961).

31. G. Herzberg and J. Shoosmith, Nature, 183, 1801 (1959).

32. G. C. Pimentel, private communication.

33. C. A. Hutchison and B. W. Mangum, J. Chem. Phys., 34, 908 (1961).

34. M. S. de Groot and J. H. van der Waals, Mol. Phys., 2, 273 (1958); 3, 190 (1960).

35. S. Foner, H. Meyer and W. H. Kleiner, J. Phys. Chem. Solids, 18, 273 (1961).

36. D. B. Chesnut and W. D. Phillips, J. Chem. Phys., 35, 1002 (1961).

37. D. B. Chesnut and P. Arthur, Jr., J. Chem. Phys., 36, 2969 (1962).

38. H. Meyer, M.C.M. O'Brien and J. H. van Vleck, Proc. Roy. Soc. (London), A243, 414 (1958).

39. J.A.R. Coope, private communication.

40. Th. J. de Boer and H. J. Backer, Rec. Trav. Chim, 73, 229 (1954).

41. R. H. Pierson, A. N. Fletcher and E. S. Gantz, Anal. Chem., 28, 1218 (1956).

42. J. A. Bell, private communication.

43. H. M. Frey, Proc. Chem Soc., 318 (1959).

44. H. S. Matheson and B. Smaller, J. Chem. Phys., 23, 421(1955).

45. D. B. Richardson, M.C. Simmons and I. Dvoretzky, J. Am. Chem. Soc., 83, 1934 (1961).

46. G. W. Robinson and M. McCarty, Jr., J. Chem. Phys., 30, 999 (1959).

47. H. M. McConnell, J. Chem. Phys., 29, 1422 (1958).

48. C. K. Jen, Formation and Trapping of Free Radicals, ed. A.M. Bass and H. P. Broida. New York, Academic Press, 1960 Chapter 7.

49. C. Heller, J. Chem. Phys., 36, 175 (1962).

50. C. H. Townes and A. L. Schawlow, Microwave Spectroscopy. New York, McGraw-Hill, 1955.

51. G. Herzberg, Infrared and Raman Spectra of Polyatomic Molecules. New York, van Nostrand, (1945).

52. J. S. Koehler and D. M. Dennison, Phys. Rev., 57, 1006 (1940).

53. F. A. Johnson and C. B. Colburn, J. Am. Chem. Soc., 83, 304 (1961).

54. L. H. Piette, F. A. Johnson, K. A. Booman and C. B. Colburn, J. Chem. Phys., 35, 1481 (1961).

55. J. B. Farmer, D. A. Hutchinson and C.A. Mc.Dowell, Fifth International Symposium on Free Radicals, July 6-7, 1961, #44

56. C. B. Colburn, private communication.

57. Air Products and Chemicals, Inc., Technical Literature on Tetrafluorohydrozine.

58. W. B. Ard, H. Shields and W. Gordy, J. Chem. Phys., 23, 1727 (1955).

59. H. N. Rexroad and W. Gordy, J. Chem. Phys., 30, 399 (1959).

60. M. D. Harmony, R. J. Myers, L.D. Schoen, D.R. Lide, Jr., and D. E. Mann, J. Chem. Phys., 35, 1129 (1961).

61. L. Pauling, The Nature of the Chemical Bond. Ithaca, Cornell University Press, 1960.

62. F. W. Brown, Phys. Rev., 44, 214 (1933).

63. D. R. Hartree and W. Hartree, Proc. Roy. Soc. (London), A193, 299 (1948).

64. J. R. Dacey, Discussions Faraday Soc., 1953, #14, 84-8.

65. T. N. Bell, J. Chem. Soc., 4973 (1961).

66, R. E. Florin, D. W. Brown, and L. A. Wall, Fifth International Symposium on Free Radicals, July 6-7, 1961, #18.

67. S.V.R. Mastrangelo, J. Am. Chem. Soc., 84, 1122 (1962).

68. S. I. Weissman and D. Banfill, J. Am. Chem. Soc., 75, 2534 (1953).